SMART CARBON NANOTUBE/FIBER AND PVA FIBER-REINFORCED COMPOSITES FOR STRESS SENSING AND CHLORIDE ION DETECTION

by

Joshua Hoheneder

A Thesis Submitted in

Partial Fulfillment of the

Requirements for the Degree of

Masters of Science

in Engineering

at

The University of Wisconsin-Milwaukee

December 2012

ABSTRACT

SMART CARBON NANOTUBE/FIBER AND PVA FIBER-REINFORCED COMPOSITES FOR STRESS SENSING AND CHLORIDE ION DETECTION

by

Joshua Hoheneder

The University of Wisconsin-Milwaukee, 2012
Under the Supervision of Professor Konstantin Sobolev

Fiber reinforced composites (FRC) with polyvinyl alcohol (PVA) fibers and carbon nanofibers (CNF) had an excellent flexural strength in excess of 18.5 MPa compared to reference samples of 15.8 MPa. It was found that the developed, depending on applied stress and exposure to chloride solutions, composites exhibit some electrical conductivity, from $4.20x10^{-04}\Omega^{-1}m^{-1}$ to. $4.13x10^{-04}\Omega^{-1}m^{-1}$. These dependences can be characterized by piezioresistive and chemoresistive coefficients demonstrating that the material possesses self-sensing capabilities. The sensitivity to stain and chloride solutions can be enhanced by incorporating small amounts of carbon nanofibers (CNF) or carbon nanotube (CNT) into composite structure. Conducted research has demonstrated a strong dependency of electrical properties of composite on crack formation in moist environments. The developed procedure is scalable for industrial application in concrete structures that require nondestructive stress monitoring, integrity under high service loads and stability in harsh environments.

TABLE OF CONTENTS

LIST OF FIGURES

LIST OF TABLES

LIST OF ABBREVIATIONS

2D	Two Dimensional
3D	Three Dimensional
AC	Alternating Current
ADS	Active Sensing Diagnostic
ASTM	American Society for Testing and Materials
CNT	Carbon Nanotubes
CNF	Carbon Nanofibers
DC	Direct Current
DOT	Department of Transportation
ECC	Engineered Cementitious Composite
EIT	Electrical Impedance Tomography
ERT	Electrical Resistance Tomography
FRC	Fiber reinforced Concrete
FRCC	Fiber-reinforced Cementitious Composite
GBFS	Granulated Blast Furnace Slag
GPa	Giga Pascal
ITZ	Interfacial Transition Zone
kN	Kilonewton
kN/min	Kilonewtons Per Minute
MPa	Mega Pascal
MWCNT	Multi Wall Carbon Nanotubes

N	Newton
NDT	Nondestructive Testing
PSD	Passive Sensor Diagnostics
PVA	Polyvinyl Alcohol (Fibers)
PCE	Poly Carboxilate Ether
SCC	Supplementary Cementitious Composites
SCM	Supplementary Cementitious Materials
SEM	Scanning Electron Microscope
SFRC	Steel Fiber Reinforced Concrete
SHM	Structural Health Monitoring
SP	Superplasticizer
SWCNT	Single Wall Carbon Nanotubes
w/c	Water to Cement Ratio

LIST OF EQUATIONS

1. Introduction

Concrete is the most used human-made material extensively applied in all for construction projects. The popularity of the material is due to its relatively low cost, high compressive strength, and relatively simple construction technology. Compared with other construction materials, concrete can resist corrosion and fire, and has a long service life. The effectiveness of concrete structures and their service life relies heavily on the reinforcement as most of the reinforcement is uncoated and deteriorates well before the concrete. When concrete is properly designed, mixed, compacted, and cured it has exceptional service life. Concrete; however, is prone to drying shrinkage cracking and micro-cracking due to service loading, which can lead to progressive increase in permeability and deterioration of reinforcement. Service life is one of the most important parameters to consider when designing and building a structure—bridges and buildings are expensive to construct, and when an aging structure fails to function properly, public expectations and even safety are at risk. The infrastructure of the United States is aging at an alarming rate. The cost of rehabilitation of existing infrastructure accounts for a large portion of the Department of Transportation's (DOT) annual budget while only about 11% is devoted to major highway construction [43]. Replacing of aging infrastructure using conventional materials and technologies relies on extensive use of Portland cement. However, the production of cement clinker is a large contributor to the world's carbon emissions at approximately 0.9 tons per ton of cement manufactured. In 1995 cement production was as much as 1.4 billion tons and has been climbing exponentially since then due to countries like China and the United Arab Emirates expanding their cites [44]. The use of high performance concrete to extend the service

life of transportation infrastructure is based on use of admixtures and supplementary cementitious materials production a very important task.

The monitoring of infrastructure conditions can allow for higher quality infrastructure and save on rehabilitation costs. Bridges need to be inspected every two years to ensure that the integrity of the structure remains in tact. Visual inspection of crack formation in structures is expensive, subjective, and elements in a structure may be inaccessible or unsafe to reach. Monitoring of structure conditions constantly for crack formation and propagation, as well as detecting the chloride ingress, is an attractive option which can reduce the inspection costs and increase safety. For example, Structural Health Monitoring (SHM) systems can be used as sensor based detection and monitoring of damage in infrastructure. Damage can be defined as any change induced to a system that has an adverse impact on the current and future performance of the system.

The constant monitoring of infrastructure will allow for a more educated approach to future designs. Currently, the standard approach to the maintenance of infrastructure is to wait until damage is visual and reactively fix the issues as they arise. Allowing for constant health monitoring during construction, setting, and the service life of the structure will allow for more proactive maintenance designs that target flawed areas as well as allow for future infrastructure to be designed to avoid these known flaws, saving money and resources while also increasing public safety.

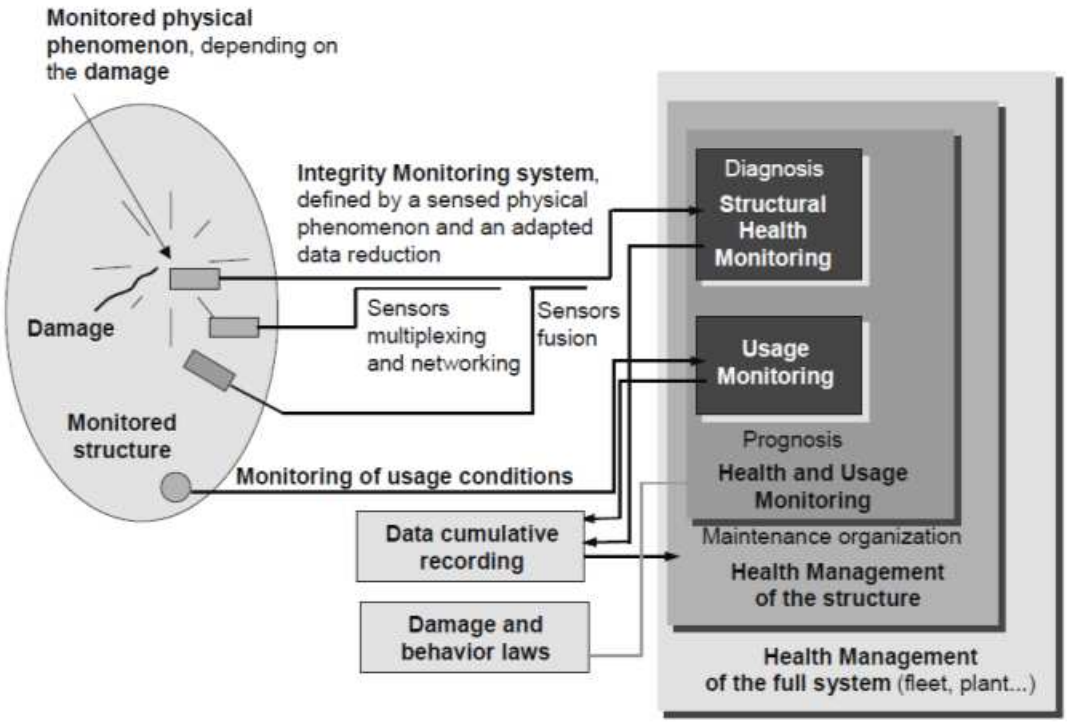

Figure 1 Principle and organization of a SHM system [45]

Advanced SHM systems can use Fiber Reinforced Concrete (FRC) for self sensing purposes. Commonly, FRCs have better durability when compared to reference concrete due to reduced drying shrinkage, pore size, increasing the electrical conductivity, increasing flexural strength and toughness [37]. Common materials used to make FRC are glass and steel fibers with some new materials such as polyvinyl alcohol (PVA) fibers, carbon nanofibers (CNF), and carbon nanotubes (CNT) just approaching the field.

1.1 Fiber reinforced concrete (FRC) for self sensing purposes

The use of admixtures and fibers in concrete mixes helps to improve mechanical properties of concrete. Water reducing agents, silica fume, granulated blast furnace slag,

and nano materials, when added to concrete mixes, result in a very dense cementitious matrix. The dense matrix, in turn, result in increased strength and durability due to reducing the capillary pores and improvement of the interfacial transition zone (ITZ) between hardened cement paste and aggregates. The ITZ is the area between hydrated cement and the aggregate. This area is weak because off the wall effect and crystallization of portlandite. The ITZ can be improved through the use of supplementary cementitious materials (SCM) like blast furnace slag (slag cement) or silica fume [34]. The capillary pores in concrete create pathways in the concrete to allow for chloride penetration. Water transports the chloride ions through the concrete and, while chlorides are not damaging to concrete directly, it causes deterioration of the steel reinforcement [47]. As steel deteriorates, its intended function of reinforcing the areas under tensile loading is no longer applicable. Other deterioration processes include freeze thaw damage which occurs by water filling the capillary pores and freezing. The freezing water expands and creates internal stresses on the hardened cement paste leading to microcracking and eventually scaling of the concrete.

Novel FRC material, Engineered Cementitious Composite (ECC) exhibits better tensile strength and ductility due to strain hardening [22]. Specifically, the addition of polyvinyl alcohol (PVA) fibers can improve the tensile strength by 2.5 times and Young's modulus by 5.8 times of the material compared with the reference samples [22]. PVA fibers have been used to improve the response under flexural loading [22,23], and cementitious materials containing a combination of PVA fibers and carbon nanofibers had gains both in strength and ductility compared with plain samples tested under flexural loading [23]. The improvement in tensile and flexural strength in PVA fiber

composites is due to the fiber's near perfect bond to a cementitious matrix. This type of FRC is a piezioresitive material that changes its conductivity in proportion to strain [16]. The effects of damage on the volume electrical resistivity in a cementitious structure is what makes the self-sensing possible. To create a self-sensing material, the use of electrically conductive materials is not necessary; however, to improve the strain- and damage-sensing capabilities, the use of electrically conductive materials was proposed [39].

The addition of electrically conductive fibers improves the conductivity of a concrete mixture. Steel and carbon fibers are electrically conductive, which help improve the conductivity of cementitious materials [7,16]. CNT and CNF based composites can serve as strain sensors [11]. The piezioresistivity of conductive fiber-reinforced cementitious composite (FRC) materials changes with strain. The strain-sensing ability is caused by the change in the volume electrical resistivity of the concrete under dynamic or static loading. This is attributed to the fiber pull-out caused by increased straining of the material [11]. Carbon fibers have been used to improve the mechanical and electrical properties of concrete [17], especially, to increase flexural strength, flexural toughness, and reduce drying shrinkage. Carbon nanofibers uniformly dispersed in a concrete matrix allow for the bridging of microcracks, which makes otherwise insulated space electrically conductive [27].

Proper design and production technology is important for "smart" FRC. This type of material incorporates the use of small particles/fibers that are used to carry load or current through the concrete matrix. For this reason, it is important to uniformly disperse the fibers within the mix. Clumping can cause adverse affects to concrete strength and

conductivity and may lead to inaccurate or false conductivity readings [10]. There have been studies conducted to ensure proper dispersion of fibers in concrete mixes [12,14,19,21]. The method of dispersion depends highly on the material to be dispersed. PVA and steel fibers are easier to disperse than CNFs and CNT and only require the use of superplasticizer mixed in water to achieve proper dispersion [24]. The dispersion of PVA and steel fibers and can be achieved using conventional mixing procedures with minimal effort. CNTs and CNFs, however, are more of a challenge to achieve proper dispersion in concrete applications. The higher degree of difficulty associated with dispersing CNT is due to the high van der Waals interacting between the CNT [38].

The fiber content must be kept below the percolation threshold to ensure high compressive strength, workability, and to reduce the material costs [46]. The percolation threshold is the critical fraction of lattice points that must be filled to create a continuous path of nearest neighbors from one side to the other [4].

1.2 Electrical conductivity

While chemical admixtures and fibers are often added to concrete to improve the durability, the use of self-sensing concrete based on carbon nanofibers/nanotubes can add additional capabilities for nondestructive monitoring of moisture conditions, chloride profiles, stresses, and crack propagation in concrete structures. Self-sensing concrete is an important component of smart buildings: structures that can detect possible failures before reaching the critical deterioration threshold can save lives and reduce the financial burdens for building owners.

Different methods for nondestructive crack detection have been proposed. Electrical Impedance Tomography (EIT) was used to detect cracking of cementitious materials under tension strain [16]; other methods include the electrical resistance tomography (ERT) [17], two and four-probe methods. The four-probe method consists of four electrical contacts on a specimen, which allows for two contacts to pass the electrical current while the other contacts detect the voltage between those points [46]. The two-probe method has two contacts on the specimen that pass the current through the cement matrix. The four-probe method is more accurate than the two-probe method because the measured resistance does not include the contact resistance [46]. Furthermore, conductivity measurements can be realized using alternating current (AC) or direct current (DC). The AC impedance investigation is a very reliable technique for nondestructive monitoring of concrete [1]; however, it requires more sophisticated equipment (i.e., network analyzers) to operate. Monitoring electrical conductivity using DC measurement, even multi-channel, can be easily realized using relatively simple data acquisition equipment [46]; however, the electrical field created during DC test leads to polarization [3]. When the centers of positive and negative charges do not coincide, the electric polarization occurs [3]. The polarization field is in the opposite direction of the applied electric field causing the polarization to increase with time during resistivity measurements. This phenomenon complicates resistivity measurements and is undesirable [3,41]. Compressive stresses decrease the length of time in which polarization occurred, and reduce the maximum extent of this effect in both plain samples and samples with of electrically conductive fibers [35].

Concrete is a nonconductive material and has a high resistance to electric current. Measuring changes in resistivity, an intrinsic property of a material, [16], will allow for the detection of crack formation and propagation. As a concrete specimen is loaded, the incurring stress creates cracks in the concrete matrix and results in air pockets. These air voids are electrically insulating and so affect the conductivity, which can be used to detect the cracks.

Electric properties can be monitored through the use of electrodes. The application of electrodes can be realized with the use of embedded or external electrodes. Embedded electrodes are utilized through the use of steel or electric wiring having been placed inside the forms prior to concrete being placed. This method is effective, however, once the structure is made, the location of electrodes cannot be altered. These embedded electrodes are higher in cost and require the implementation by trained professionals to ensure proper installation. External electrodes have the distinct advantage of being placed after the structure is already built. While structures with embedded electrodes cannot be altered once constructed, external electrodes can be placed and changed throughout the service life of the structure. When an electrode no longer functions properly on a structure with external electrodes, the electrode can be easily fixed or replaced without the need to damage the structure. Ease of implementation and relative cost savings associated with externally applied electrodes make it an attractive option for SHM applications.

1.3 Loading on structures

Concrete used as structural elements is exposed to many types of loading conditions during its service life. Service loads experienced in a structure range from design loads, fatigue loading, and failure loading. The research conducted aimed to study two loading conditions that were most likely to lead to failure. These two conditions were the fatigue due to repetitive loading and mechanical loading until failure.

Most structures experience repetitive loading that vary over time due to wind loads or live loads. An example of repetitive loading on bridges is the dynamic loading of cars transferring from the approach slab to the bridge deck. In this area, there is often an elevation change that causes the vehicle to place a dynamic load on the structure from the weight of the vehicle pushing on the struts of the car and transferring this load into the bridge deck. For this reason, testing samples under repetitive or cyclic loading was an initial consideration in the design of this experiment.

Most structures do not ever experience or exceed the design loads on a structure because they are designed with a factor of safety to account for different loading conditions that are not accounted for during the design process. While the overall structure may never experience design loads, there may be certain elements/zones of the structure that do experience the excessive loads and, therefore, experiment was designed to account for these loadings.

The purpose of this experiment was to determine whether the proposed procedure would lead to the detection of stresses and cracks in a concrete element. Loading until failure for concrete specimens was necessary to ensure crack development and progress. Under cyclic loading, the specimens were tested within their elastic zone so crack

formation was minimal and, therefore, loading until failure was essential in this testing program.

1.4 Objectives

1.4.1 Justification

To ensure public safety, structural elements are inspected on a scheduled basis with an average frequency of two years. It is not cost or time effective to inspect the entire structure so areas of highest concern are inspected more thoroughly. In service structures, however, can suffer deterioration or damage in areas that are not inspected. Unexpected damage can be caused by the formation of cold joints, improper construction practices, or flawed construction materials.

The cost associated with inspections of structures is often the limiting factor for inspection frequency. Since damage to a structure can happen at any time, the structural integrity between inspections is often left in question. Developing a method to continually monitor structures will increase public safety as well as save on inspection costs.

1.4.2Research objectives

The objective of this work was to prove the concept of monitoring the changes in conductivity in structures as a structural health monitoring (SHM) system. To achieve this objective, research was conducted on the behavior of electrical current under mechanical loading. Concrete has the ability to conduct electrical current and through the

use of electrically conductive additives, this ability can be enhanced. The objectives of this work were achieved by implementing the following work tasks.

- Task 1: Research behavior of electrical conductivity under mechanical loading.
- Task 2: Research electrode alternatives for monitoring conductivity in samples.
- Task 3: Test the concept under various loading and moisture conditions.
- Task 4: Gather and present conculsions.

2. Literature review

Reinforcing concrete with steel rebar is a standard technique used in modern construction. Concrete has high strength when loaded in compression; however, when loaded in tension the strength is assumed to be zero in designs. Steel rebar is strong under tensile loading and is added to concrete to increase span lengths and design loadings for beams, columns, floor slabs, and other structural elements.

Concrete under flexural tensile loading is subject to crack formation and propagation. The standard method for crack monitoring is through the use of visual inspection. Bridges need to be inspected biannually to ensure the integrity. Visual inspection is subjective, time consuming, expensive, and often dangerous due to the location of the structural element. Developing a way to monitor concrete conditions remotely, constantly and in a nondestructive manner is a very attractive option.

Corrosion of steel reinforcement is caused by water and chloride penetration through the concrete. Corrosion of steel leads to a loss of strength, and rusting causes volume changes within the concrete matrix. The volume changes lead to cracking and debonding of the steel and concrete. Designs and structural performance depend on the bond between concrete and steel to predict strength. The reduced bond decreases overall strength and performance of the structure. Concrete reinforced with fibers has been used as an alternative to secondary steel reinforcement. FRCs which uses non corrosive fiber materials is considerably lighter than steel reinforced materials, reducing the weight of a structure.

2.1 Nondestructive monitoring: current methods

Nondestructive monitoring of concrete has been a major research topic for years. There are many methods developed for this purpose including C-scan, x-ray, eddy current, and coin tapping [35]. These methods, while effective, are often time consuming, labor intensive, and impractical for in-service conditions.

There are two categories of SHMs: Passive Sensor Diagnostics (PSD) and Active Sensing Diagnostic (ADS) [35]. PDS uses passive senor measurements to determine changes in condition or environment of structures. ADS measurements can identify damage by analyzing the differences in sensor signals before and after the damages are induced [35].

Of the above mentioned techniques for nondestructive monitoring of concrete many fall into the PDS method: coin tapping, x-ray, c-scan, and other methods are types of PDS monitoring and are conducted onsite to determine extent of damage experienced during the service life of structure. PDS techniques can be used on existing structures and don't need to be incorporated during construction and design [35].

2.1.1 Coin tapping

Coin tapping is a method of nondestructive monitoring of concrete structures through the use of acoustic sound response. The test can be used to detect poor quality concrete, debonding of overlays or applied composites, corrosion of reinforcement, or global softening. ASTM D4580 - 03(2007) Standard Practice for Measuring Delaminations in Concrete Bridge Decks by Sounding, covers the evaluation of affected concrete using sounding techniques [2].

Acoustic testing of concrete has many applications in NDT on structures. A major advantage is that it produces immediate results on near surface defects. While these results are immediate, the results are highly depended on the operator [2]. These tests cannot be conducted in inaccessible areas and so require for an inspector being present in dangerous areas.

There are many methods to conduct acoustic testing of concrete deficiencies. These tests include coin tap, chain drag, hammer drag, and an electro-mechanical sounding device. Each of these tests utilizes nondestructive testing for monitoring of the concrete; however, the coin tap test is one of the oldest and most widely used methods. The test requires the inspector to tap on the concrete sample with a small hammer, coin, or some other rigid object while listening to the sound resulting from the impact. The difference between the sounds created during the tapping is what allows for the determination of damage. When concrete creates a clear ringing sound upon impact, the test indicates that there is little or no problem with damage. Concrete that has issues with strength or debonding will have a dull or hallow sound when struck with the object. The difference in sound is due to a change in the effective stiffness of the concrete, resulting in frequencies of an impact differ between areas of good and poor quality concrete.

2.1.2 Ultrasonic testing

Ultrasonic (sound having a frequency above 20,000 hertz) testing is another effective NDT method for concrete testing. Testing of materials using ultrasonic techniques utilizes the vibrations of the material that comprise a given medium [2].

Ultrasonic testing can used on a variety of materials including, but not limited to: metals, rock, concrete, liquids, and various nonmetals. It can be used for non-destructive detecting internal damage and deterioration in concrete. These flaws include deterioration due to sulfate and other chemical attacks, cracking, and changes due to freeze-thaw cycling [2].

The ultrasonic method is used to obtain the properties of materials by measuring the time of travel of stress waves through a solid medium. Ultrasonic method requires equipment to emit stress waves through the concrete and uses a separate device to measure the time it takes for the waves to travel through it. The time it takes for a stress wave to travel can then be used to obtain the acoustic velocity of a given material. The acoustic velocity can enable inspectors to make judgments as to the integrity of a structure [2].

Figure 2 A portable ultrasonic testing device [49].

Ultrasonic monitoring of construction materials delivers reliable readings of the instu conditions of buildings. This method, however, is time consuming and impractical for global inspection. It is also not cost effective due to the high cost of using trained professionals to operate the equipment and to ensure the integrity of the readings.

Elimination of the need for inspectors to reach inaccessible or dangerous areas is not accomplished in this test method [2].

2.1.3 Electric current induction

This test is an extension of the magnetic field perturbation method, also known as the eddy current method. For this method to work, the material being explored needs to be electrically conductive, but not magnetically permeable. An electric current is induced between two points and affected areas are identified by recording the magnetic field signals [2].

This method is not effective as a direct monitoring technique of NDT. Concrete is a nonmagnetic material and the use of magnetic fields to identify problem areas has not proved to be a reliable technique. This technique, however, is effective for monitoring embedded steel or prestressing tendons [2].

2.1.4 Radiography

Radiograph is defined as an image produced on a radiosensitive surface, such as a photographic film, by radiation other than visible light. The most common form of radiation used are X-rays, however, Gamma rays are also used. The two forms of radiation used differ by the wave lengths. These are considerably shorter than that of visible light about 1/10,000 and 1/1,000,000 the length of visible light waves, respectively [2] which allows for the penetration of most materials by these waves. Instruments needed for conducting this test are radioisotopes or X-rays acting as a wave source and photographic film which acts as a detector [2].

Testing using radiography is a great way to get an accurate portrayal of the damage that has occurred to a structure. Radiography is only used in areas that all surfaces of the structural element are exposed because of the need to have the wave emitter on one end and the film on the receiving end. For this reason columns and wall elements are great candidates for this test method, however, the foundation and floor slabs can't be tested. This test uses an expensive instrumentation, requires the use of a trained professional onsite to handle the equipment and make judgments, and also is limited by accessibility. Due to the radiation that is emitted during the testing of construction materials, safety to the inspector and the public is a major concern, making this test impractical in many situations [2].

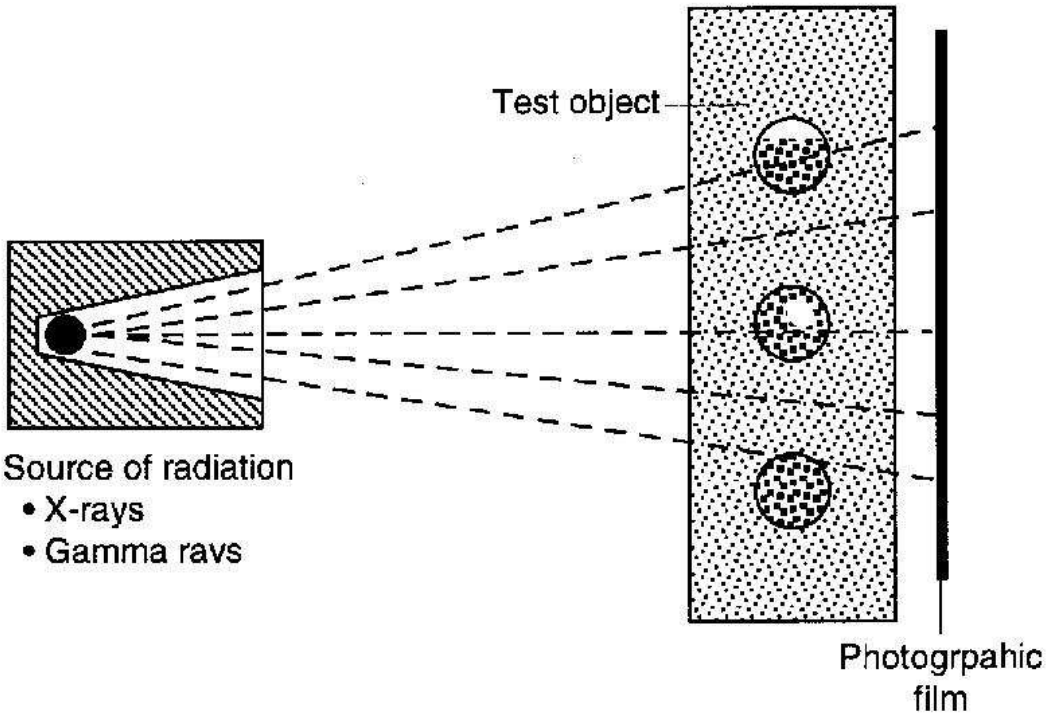

Figure 3 Schematics of radiography [2]

2.2 The use of stress-sensing materials

The construction industry has been going through a change in philosophy. High rise buildings are becoming more common in large cities with the higher population sizes and low availability of land. In the past high rise buildings were built with large columns and larger ceiling heights. Recently there has been a move to reduce the size of floor slabs and columns to reduce the need for taller buildings and increase useable floor space [24].

To reduce the size of columns and floor slabs the use of high strength concrete has been a popular solution. High strength concrete has lower permeability than normal strength concrete for this reason it performs better under harsh climate conditions. As concrete gains higher compressive strength, it loses ductility. The incorporation of fibers into concrete mixes allows for reduction size of concrete elements such as columns and floor slabs.

2.2.1 Steel fibers

Concrete with steel fiber reinforcement has improved flexural strength, fracture toughness, thermal shock strength, and resistance under impact and fatigue loadings. Cracks that form in the concrete matrix are bridged by these fibers and are restrained from propagating [24].

The addition of fibers to concrete results in a loss of workability. Fluidity of concrete during placement is important because there is a need to ensure that the concrete reaches all parts of the form evenly. Steel rebar, especially in the corners of buildings, can be packed close together and placing concrete in these areas with an unworkable concrete may be impossible. There are multiple approaches that can be employed to

improve the workability of concrete. Increasing fine aggregate content or adding water reducing agents are some of the most effective ways to maintain the concretes workability for construction purposes [26].

Steel Fiber Reinforced Concrete (SFRC) has good mechanical and electrical properties. Figure 4 demonstrates that with the addition of steel fibers, compressive strength remained mostly unaffected while the post-cracking behavior was considerably different. The cracks in the concrete are bridged by the fibers leading to smaller, more evenly distributed cracks in the side loaded in tension. The failure of SFRC under flexural loading is not a sudden failure as in plain concrete, but controlled and delayed [26]. When used in a structure, the excessive deformation before failure would allow for a greater warning before ultimate failure of the structure.

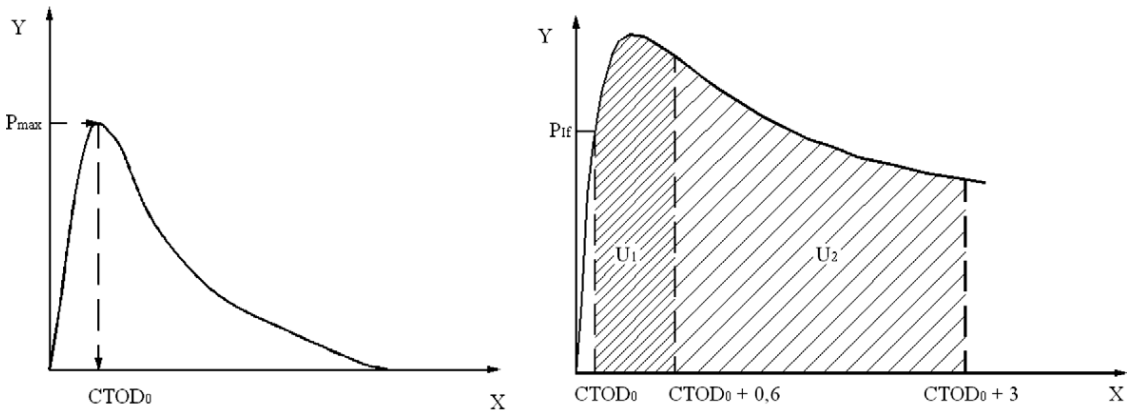

-a -b

Figure 4 (a) Basic concrete load–CTODm diagram: CTOD0 meaning. (b) Load–CTOD diagram: U1 e U2 determination. [26]

2.2.2 The use of PVA fiber reinforced ECC

The use of polyvinyl alcohol (PVA) fibers in concrete has been the topic of much research. In the past, it was believed that in order to improve the ductility of concrete, the strength of concrete matrix must be reduced. With the addition of PVA fibers into

concrete designs, the strength of the material does not have to be reduced to improve ductility.

Once plain concrete suffers initial cracking under flexural loading, the failure is very sudden. Concrete reinforced with PVA fibers can continue to gain strength after initial cracking occurs due to strain hardening. Strain hardening FRC materials are characterized by their ability to sustain increasing loads after initial cracking [33]. Past research focused on using large volumes of fibers, typically in the range of 10 to 20% by volume; however, the same performance can be achieved with only 2% by volume of PVA fibers [33].

A group of researchers studied the effect that different size PVA fibers on the performance of ECC [19]. Two different PVA fibers were considered. The first had a diameter of 0.66 mm and a length of 30 mm, while the second had a diameter of 0.10 mm and a length of 12 mm. Results from this study determined that the main factor affecting the properties of the mixtures is the surface area of the fibers. When the same volume of fibers is used, the smaller fibers are going to have an overall larger surface area and therefore have a greater bond with the cementitious matrix. This can, in turn, create a better opportunity for multi-cracking and strain hardening behavior.

2.2.3 Carbon nanofibers

CNFs have been an advanced research subject since their discovery. The material is being considered in many different applications due to its unquie mechanical and electrical properties. The mechanical properties of CNFs include a high tensile strength of 12,000 MPa and a high Young's modulus of 600 GPa. Comparing the mechanical properties, CNFs are approximately 10-20 times stronger than steel [20]. The great

mechanical properties have lead to research on incorporating the CNFs into different materials, including concrete.

The use of CNFs in concrete is a relatively new approach. CNF has had limited applications due to the high production costs associated with the material. Recently, however, the production costs have been reduced due to better techniques being developed for production of larger quantities of CNF material and so the use of CNFs became a feasible option in reinforcing concrete (Figure 5).

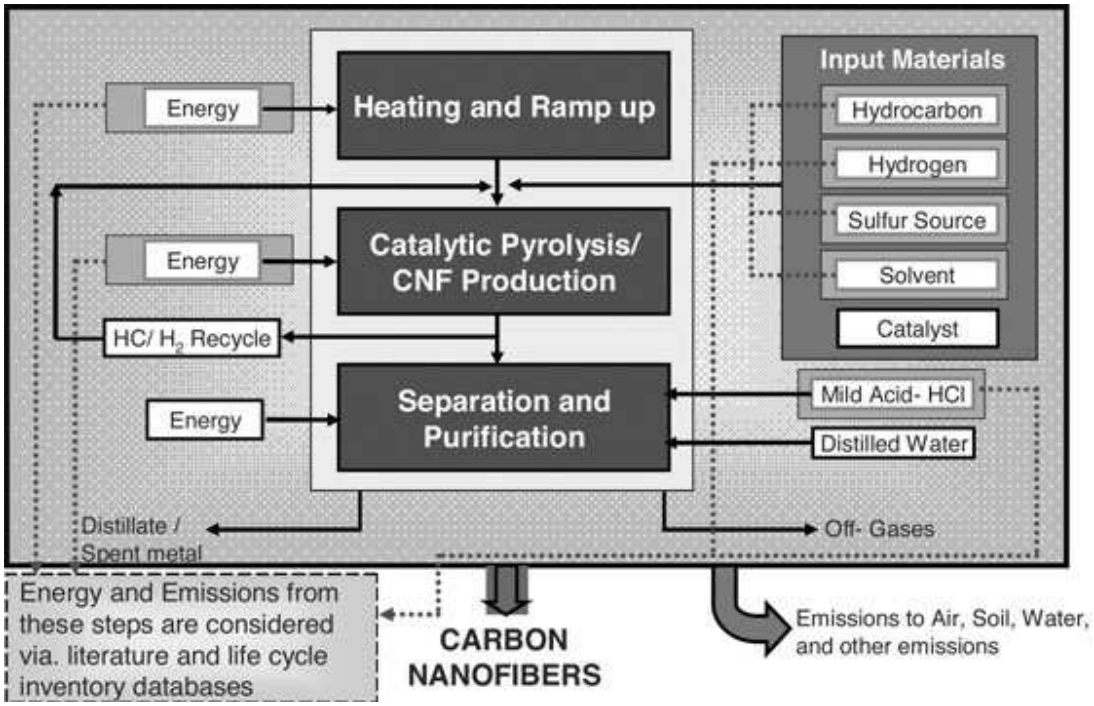

Figure 5 Vapor-grown carbon nanofibers–life cycle assessment (VGCNF-LCA): system boundary [20]

The leading cause of steel corrosion varies by geographic regions. To corrode steel, the pH is needed to be reduced. This can happen due to carbonation of concrete in some areas of the country while chloride attack carried by water through the concrete is

the leading cause of steel corrosion in other geographic regions. Chlorides can travel directly to the steel reinforcement through capillary pores created by cement hydration. The pores affects on concrete durability can be reduced through the use of smaller particles the filling of voids created by interfacial transition zone (ITZ) between larger cement particles with smaller particles or by reducing the water to cement ratio. CNFs are perfect for this because of their size and shape. CNFs have diameters that range from tens of nanometers to 200 nanometers allowing for these small pores to be filled creating a denser concrete matrix [20]. Advantages gained in the concretes performance include increasing in the tensile and flexural strengths, tensile ductility and flexural toughness, and decreases the drying shrinkage [41]

Electrical properties of CNFs make it an ideal candidate in the use of nondestructive monitoring of structures. When added to concrete, CNFs give the material a strain-sensing ability also called self-sensing concrete [41, 46]. Self-sensing concrete is made possible by the decreased electrical resistivity caused by the addition of the electrically conductive CNFs. Since concrete is a semi-conducting material, a decrease in resistivity occurs even when fibers are at a volume below the percolation threshold [41]. Damage to concrete creates an increase in resistivity by increasing the void size in the concrete matrix [46]. Void spaces are electrically insulating areas and lead to an increase in resistivity which can be measured and interpreted as damage. Short CNFs are preferred to long CNFs because of the inherent need to keep material costs low, increase workability, and ensure high compressive strength [41].

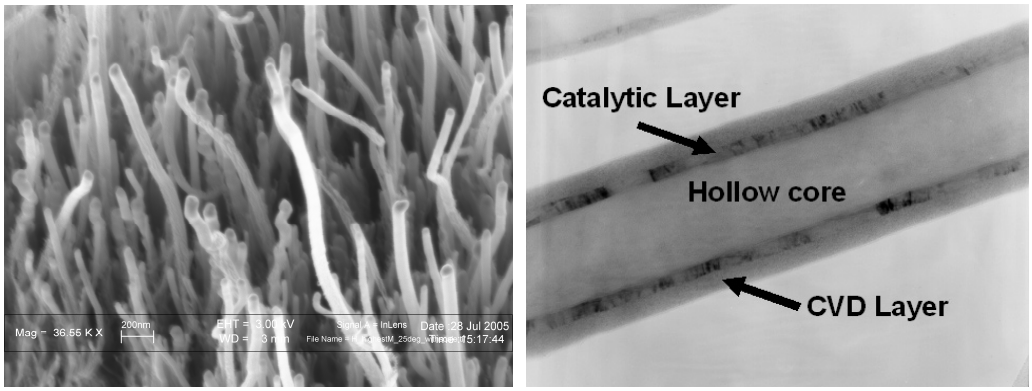

Figure 6 SEM of CNF [28]

2.2.4 Carbon nanotubes

In addition to steel and carbon nanofibers, carbon nanotubes are a great candidate to improve the properties of concrete. CNTs were discovered by Iijima in 1991 [47]. The material is being considered in many different applications due to its mechanical and electrical properties. There are two main types of CNTs, single wall carbon nanotubes (SWCNT) and multi wall carbon nanotubes (MWCNT).

CNTs act much like CNFs when added to concrete mixes. The fibers allow for the bridging of microcracks, the reduction in porosity, reduction in shrinkage cracking, and control the cracks in concrete at the nanoscale [46]. The MWCNTs can strongly modify C-S-H and reinforce the nanostructure of the cementitious matrix by increasing the amount of stiffness [14].

There are many differences between the two types of CNTs. The differences stem from the production process between the two CNT types creating basic or more advanced structures. SWCNT have many properties that are make them a great candidate for the inclusion in concrete designs. Due to their one dimensional, all carbon structure SWCNTs have great mechanical, thermal, and electrical properties [38]. SWCNTs are

typically bundled mixtures due to strong inter-tube van der Waals interactions and hydrophobic interactions. These fibers have a lot of potential for composite applications for self sensing capabilities [38]. MWCNT give similar results as SWCNTs when added to concrete. Both types have excellent mechanical and electrical properties, the differences between the two types come more from the production and the physical formation of the tubes themselves. Mechanical properties of SWNT usually exceed those of MWNT; therefore, measurements of Young's modulus give results in the range of 1,000 GPa and 500 GPa, respectively [32].

2.2.5 The dispersion of fibers/ nano materials

Fiber reinforced concrete has many advantages when compared to plan concrete. These advantages include improvements in mechanical and electrical properties when mixes include CNF/CNT. When fibers are added to concrete, two major problems are observed, workability of concrete is lowered and fibers tend to agglomerate. Numerous research studies were conducted to reduce or eliminate these limitations.

The dispersion of fibers into concrete elements affects the properties of the composite. Poor dispersion of fibers can lead to adverse effects in the performance and so limiting the efficiency of the fibers in the matrix [12]. These defect sites are areas of lower strength and also create a discontinuity in matrix affecting both the mechanical and electrical properties of the concrete.

The dispersion of steel and PVA fibers can be achieved in little time with minimal effort. CNF and CNTs, however, are more of a challenge to achieve proper dispersion in concrete applications. The higher degree of difficulty associated with dispersing CNF/CNT is due to a high aspect ratio [29] and the high Van der Waal forces interacting

between the CNF/CNT [38] making them prone to entanglement and bundling. The adjacent CNTs can have an interaction energy of ca. 500 eV/μm of tube–tube contact [29]. The strong interactions between the individual fibers create a need to break these bonds before the dispersion is achieved.

There are many methods to properly disperse fibers into concrete. Dispersion techniques include both chemical and mechanical approaches [29]. Mechanical methods include using high-shear, high speed or ultrasonic mixing, and ball milling.

The production of various fibers causes an entanglement of fibers that must be corrected before proper dispersion can be realized [29]. The destruction of attractive forces can be achieved through mechanical methods such as ultrasonication or ball milling the fibers [14]. This method is effective for dispersing the fibers; however, the fibers become fractured and broken. Ball milling and ultrasonification will help to break the Van der Waal forces by creating shorter, fragmented tubes that have less strong natural attractions by reducing their aspect ratio. Dispersion using this technique leads to an unstable, poorly dispersed product [29].

Chemical methods for fiber dispersion are an attractive method for creating a uniform dispersion in concrete. Enhancing the mechanical properties of materials such as strength, toughness, reduction in porosity, and ductility can be achieved through the use of surfactant admixtures that are used to disperse the fibers into concrete. Creating a method that optimizes the combination of admixtures and fibers in the concrete is the most important consideration in CNF/CNT based FRC. Chemical processing of fibers include, but are not limited to: use of superplasticizer, acid treatments and addition of silica fume.

The first method is to use surfactants such as superplasticizer in order to disperse the fibers in concrete. Superplasticizers change the surface energies to reduce the attractive forces between fibers helping to keep the fibers suspended [29]. Those amphiphilic molecules, compounds having both polar and apolar groups, act to reduce the surface tension. The surfactants structure consists of two parts, the head and the tail (Figure 7).

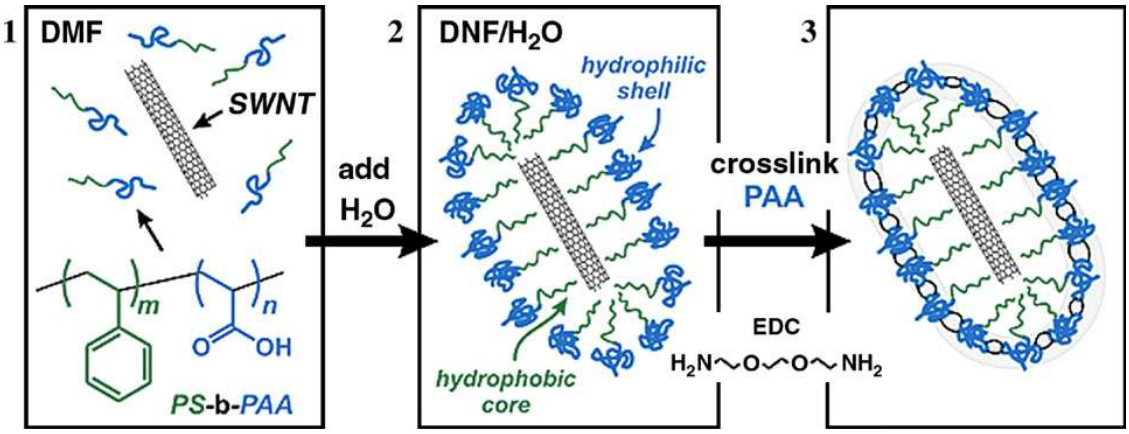

Figure 7 The general strategy for encapsulating SWNT within shells of amphiphilic block copolymer PS-b-PAA [32]

The head is known as the hydrophilic region while the tail is known as the hydrophobic. The tail portion of the surfactant usually consists of hydrocarbon chains. Surfactants are classified according to the charge of their head groups, thus cationic, anionic, or nonionic [32]. The surfactants used do not completely disperse the fibers alone in water, so using ultrasonic mixing is an option to facilitate the dispersion [29]. A surfactant's property of accumulation at surfaces or interfaces has been widely utilized to promote stable dispersions of solids in different media The second option is to use silica fume in addition to superplasticizer to help break apart the attractive forces between particles to create a more uniform dispersion. Silica fume has a particle size around 100-

500 nm and, when added to concrete, improves the density (filler effect) and therefore causes the permeability to decrease [30]. The reduction in permeability improves the corrosion resistance of embedded steel rebar [41].

The method of acid treatment is also effective for the dispersion of CNT. CNTs can be dispersed in water using a couple of different acids. The two acids used most often for the surface treatment of fibers are sulfuric acid and nitric acid. During the reaction of the acid and CNTs, oxygen atoms from the acid react with the carbon atoms on the nanotubes. The reactions are more common at the ends, curvatures, and defect sites on the CNT. Negatively charged carboxylic groups will be introduced on the CNT surfaces as a result of the oxidation. The repulsion forces between the negative charges that are associated with the individual CNT are used to disperse the fibers without the use of surfactants [47].

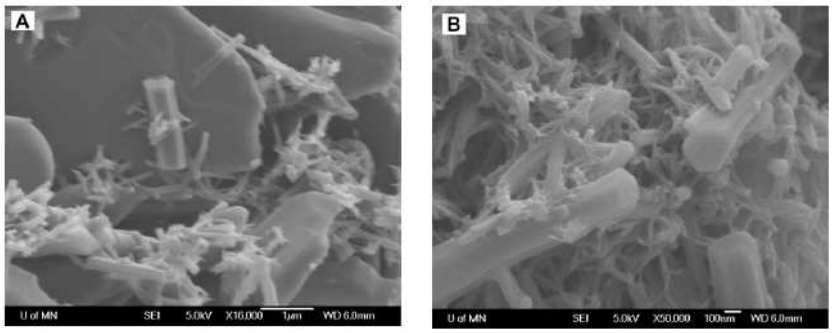

Figure 8 SEM (scanning electron microscope) pictures of CNT/cement composites after acid treatment. Untreated (left) and Treated (right) [47]

2.3 The use of AC and DC for NDT

NDT can be realized using a wide range of different techniques. The technique used in this research relies on the changes in conductivity of the material. NDT can be accomplished using stress-sensing materials through data acquisition systems to

continually monitor the cracking through conductivity. Cracks are void space in the concrete system that are electrically insulating and create a change in conductivity that can be monitored [46]. Alternating Current (AC) and Direct Current (DC) testing techniques can be utilized for NDT with smart materials.

Investigating conductivity can be realized using (AC) or (DC). Sensing by AC impedance measurement is less popular than DC resistance measurement because the DC method is easier for implementation [46]. The AC impedance investigation is a very reliable technique for nondestructive monitoring of concrete [1]; however, it requires more sophisticated equipment (i.e., network analyzers) to operate. More sophisticated equipment is more expensive to produce, own, and operate a SHM system. The additional costs often lead to this technique to not be implemented.

2.3.1 Techniques used

The NDT technique that is being tested in this research involves passing electrical current through concrete and monitoring its change under mechanical loading. Different techniques that have been studied in the past are Electrical Impedance Tomography (EIT), used to detect cracking of cementitious materials under tension strain [16], the two-and four-probe methods, and electrical resistance tomography (ERT) [17].

The EIT technique has been studied by Tsung-Chin Hou at the University of Michigan, Ann Arbor. This technique was proposed for measuring the internal strain fields of concrete on the boundary of the structure. This technique works well in both two dimensions (2D) and three dimensions (3D) for measuring the strain fields in a concrete element. Reductions in conductivity are mapped and imaged through this

technique. EIT is designed to work both with plain concrete as well as FRC. Another advantage to this technique is that it can be used on existing structures since it uses external electrodes to take its readings. This method of testing uses alternating current and requires that AC excitations be greater than 100 Hz [16].

The ERT method of monitoring changes in conductivity is an effective way to probe for crack formation. This method applies the AC into the specimen to gain a 3D image of the damage. Electrodes are attached to the surface of the concrete specimen to measure the voltage across the surface. These boundary measurements are used for reconstructing the internal conductivity distribution taking into account the geometry and the spatial variations of the conductivity [17]. Figure 9 displays the ERT set up for a tested sample. Embedded in the sample is an electrically insulating material which is used to produce a contrast in the material in respect to conductivity. This figure shows how even though the sample is comprised of concrete in all other areas, the conductivity is not consistent. This is due to the porosity of the concrete. The pores are not of equal size or distributed so different factor,s such as moisture absorption, are not consistent throughout the sample causing differences in conductivity. The EIT and ERT techniques require sophisticated equipment to conduct and a trained professional to monitor the tests, significantly increasing the installation and operation costs

.

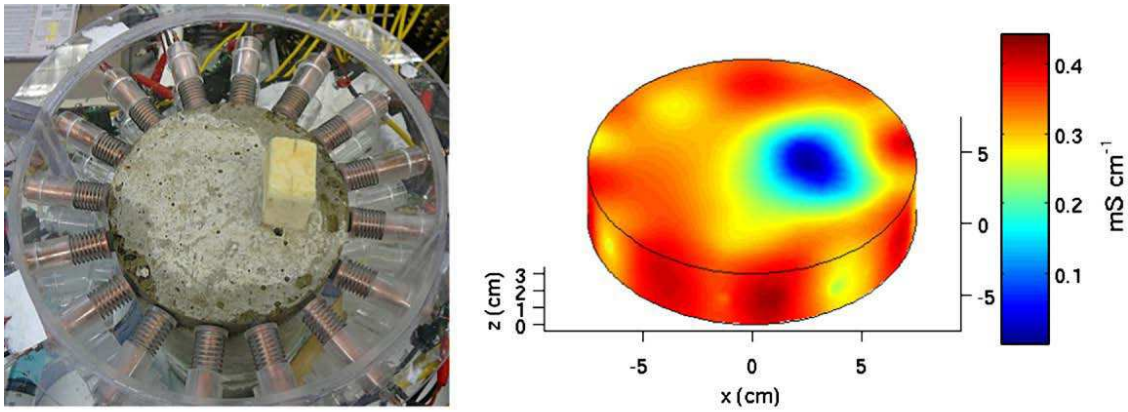

Figure 9 a) A specimen with attached electrodes. b) The ERT reconstruction. [17]

The two and four probe methods are effective and relatively simple methods for monitoring conductivity in concrete specimens. The four-probe method consists of four electrical contacts, which allows for two contacts to pass the electrical current while the other contacts detect the voltage between those points [46]. The two-probe method has two contacts at the end of the specimen that pass the current through the cement matrix. The four-probe method is more accurate than the two-probe method because the measured resistance does not include the contact resistance [46]. Furthermore, investigating conductivity can be realized using alternating current or direct current. When DC is applied to a specimen, the conductivity can be calculated through the following equation [16].

$$\sigma = \frac{I * L}{V * w * h} \quad \textbf{[1]}$$

Where:

L: Electrode Spacing (m)
w: Specimen Width (m)
h: Specimen Height (m)
I: Electrical Current (amp)
V: Voltage Drop (Volts)

It was found that the compressive stress in a concrete specimen greatly reduced the extent of electric polarization in samples [35]. Polarization occurs in the sample as well as at the contact areas of the electrodes. These effects are also different when comparing the two and four probe methods [41].

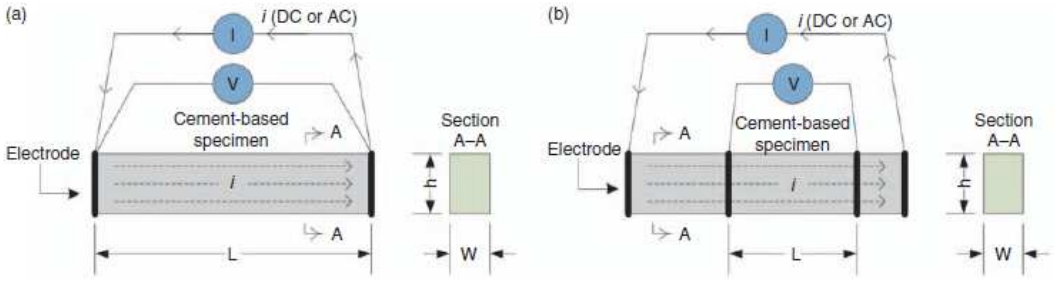

Figure 10 Conductivity measurement based upon a) 2-point and b) 4-point probe technique [16]

When polarization occurs at the interface between cement and the electrical contact, the two probe method is used to limit these effects. The four probe method is used when the polarization occurs within the cement to limit the polarization effects [3]. Polarization effects are reduced with the increase in temperature. This reduction is due to the activation energy involved in electrical conduction [3]. Increased compressive stresses decreased the length of time in which polarization occurred, and reduced the

maximum extent of this effect in both plain samples and samples with the addition of electrically conductive fibers [35].

2.3.2 Electrodes: Embedded vs. External

Electrodes are used to measure the conductivity across concrete specimens for the nondestructive monitoring of concrete structures. Electrodes can be made with different materials including, but not limited to stainless steel [46]. The electrodes can be embedded in the concrete or attached to the surface of a specimen. Embedded electrodes have the advantage of being protected from the environment from the concrete cover; however, they cannot be added once the structure is complete. External electrodes can be fixed or replaced if an electrode is damaged as needed. Another advantage to using external electrodes over embedded electrodes is that they can be added to existing structures easily and in a cost effective manner. The electrodes can measure the changes in conductivity from any initial reading. The measurements cannot analyze existing damage, but it can analyze new damage formation and propagation from mechanical loading.

3 Experimental Procedure: Materials and methods

3.1 Materials

3.1.1 Cementitious materials

The cement used for this experiment is Type I portland cement produced by Lafarge North America. The chemical and physical properties of the cement are listed in Table 1.

Table 1 Properties of portland cement and ASTM C150 requirements

CHEMICAL			PHYSICAL			
Item	**Spec. Limit**	**Test Result**	Item		Spec. Limit	Test Results
SiO2 %	--------	20.6	Air content, % (C-185)		12 max	7.5
AL2O3 %	--------	4.7	Blaine fineness, m2/kg (C-204)		260 min	380
Fe2O3 %	--------	2.7	Autoclave expansion, % (C-151)		0.8 max	0.02
CaO %	--------	63.9	Compressive Strength, MPa			
MgO %	6.0 max	2.3		1 day	---------	12.4
SO3 %	3.0 max	2.4		3 days	12.0 min	21.7
Ignition loss %	3.0 max	2.1		7 days	19.0 min	27.6
Insoluble residue %	0.75 max	0.36		28 days	28.0 min	37.9
Free lime %	--------	1.1	Time of setting, minutes			
CO2 %	--------	1.3		Initial	45 min	110
Limestone %	--------	3.4		Final	375 max	225
CoCO3 in limstone %	-------	93.0	Heat of hydration at 7 days, kJ/kg		---------	411
Potenial, %			Percent Passing 325 Mesh (C-430)		---------	95.4
C3S %	--------	55.0				
C2S %	--------	17.6				
C3A %	--------	8.0				
C4AF %	--------	8.2				
C3AF+2(C3A) %	--------	24.2				
C3S+4.75(C3A) %	--------	93.0				
Na2Oequi %	0.6 max	0.55				

3.1.2 Chemical admixtures

To improve the workability of the mixture while maintaining the low water and cement ratio, a high-range water-reducing admixture (polycarboxilate PCE from Handy Chemicals Montreal, Canada) was added to the mixture at a dosage of 0.125% by weight of cement.

3.1.3 Fibers

There are two different types of reinforcement used in this research: PVA and CNF/CNT. All samples that were tested contained PVA fibers. Kuralon K-II PVA fibers from Kuraray Japan have the dimensions of RECS 7x6 mm. The fibers mechanical and geometric properties are summarized in Table 2. The fibers were added to the concrete in the proportion of 3 percent by volume for the initial study.

Table 2 Properties of PVA fibers

Fiber Length (mm)	Length (mm)	Thickness (dex)	Diameter (mm)	Youngs's Modulus (kN/sq. mm)	Tensile Strength (GPa)
RECS 7x6 mm	6	7	0.027	39	1.6

While reference samples contain only PVA fibers, experimental samples contain other typs of fibers. The two different kinds of fibers studied include carbon nanotubes and carbon nanofibers. The carbon nanofibers are PR-24-XT-PS and are produced from Pyrograf Products while the carbon nanotubes were produced by Eden Nanomaterials. The additions of these fibers were incorporated to increase the electrical conductivity and increase the flexural strength. The CNTs and CNFs were added to the mix in the ratio of 0.2 percent by volume. Table 3 and Table 4 summarize the mechanical and geometric properties of the types of the CNF and CNT respectively.

Table 3 Properties of Carbon Fibers PR-24-XT-PS

Fiber Diameter, nm (average):	CVD carbon overcoat present on fiber	Surface area, m2/gm:	Dispersive surface energy, mJ/m2:	Moisture, wt%:	Iron, ppm:	Polyaromatic hydrocarbons, mg PAH/gm fiber:
100	Slight	45	85	< 5	< 14,000	< 1

Table 4 Properties of Carbon Nanotubes

Diameter (nm)	Purity (% carbon by mass)	Bulk Density (g/cm^3)
20-30	95	0.107

3.1.4 Standard silica sand

Standard graded silica sand conforming to ASTM C778 and AASHTO 106 was used in the research program. This sand is graded between No. 30 and No. 100 sieves and was supplied by US Silica Co, Ottawa, IL. Typical grading values for this silica sand can be seen below (Table 5).

Table 5 Typical grading of standard silica sand

USA STD Sieve size		Typical Values		
		% Retained		% Passing
Mesh	Millimeters	Individual	Cumulative	Cumulative
16	1.180	0.0	0.0	100.0
30	0.600	2.0	2.0	98.0
40	0.425	28.0	30.0	70.0
50	0.300	45.0	75.0	25.0
100	0.150	23.0	98.0	2.0
PAN		2.0	100.0	0.0

3.2 Mixture proportions

The water to cement ratio (w/c) used for the experimental mixtures was 0.3. This was done to keep a dense concrete with little electrically insulating air voids to allow for

the free flow of electrical current in the system. Silica sand was used at a sand-to-cement ratio of 0.5.

Table 6 Mixture proportions used in the preliminary study.

Composition	Reference FRC	CNF PVA-FRC
W/C	0.3	0.3
S/C	0.5	0.5
SP, % w cement	0.125	0.125
PVA fibers, % vol	3	3
Carbon nanofibers, %vol	0	0.2

3.3 Mixing procedures

3.3.1 Mixing procedure for PVA-ECC

The mixing procedure for PVA-ECC mix with CNT/CNF is important. Avoiding the agglomeration of fibers can yield the highest quality specimens possible. Different mixing procedures were conducted to determine what would lead to the least agglomeration of fibers in the samples. Samples were mixed in a 20 quart Hobart HL-200 mixer (Figure 11). Common mix procedures led to the fibers clumping up into a ball so to avoid this, the mix procedure was adjusted to the following.

The dispersion of the CNFs/CNTs was done in water with PCE (and silica sand) as listed in 3.3.2 and 3.3.3. Portion (75%) of the water was added to the bowl of the Hobart mixer with silica sand and mixed at low spped (107 rpm) for 30 seconds. After the sand and water were mixed, half of the PVA fibers were added and mixed for 30 seconds at low speed. Once that was completed, the rest of the fibers were added and mixed at the same speed for an additional 30 seconds. Half of the portland cement was

added to the mix for 30 seconds at low speed, followed by the second half at the same speed. The rest of the water, PCE, and CNF (or CNT) was added and mixed at low speed for 30 seconds then for another 30 seconds at medium (198 rpm) speed. The workability of the mix was tested on the flow table and then remixed for an additional 30 seconds at medium speed before being placed into molds.

Figure 11 Mixing of PVA-ECC using Hobart mixer

Once the ECC was mixed, the specimens were cast. Two types of specimens were used for compressive and flexural testing. The specimens cast for compressive testing were cast into cube molds that had the dimensions of 50.8 x 50.8 x 50.8 mm and the specimens tested for flexure were cast into 14 x 40 x 160 mm. The molds used are pictured in Figure 12.

Figure 12 Molds used for sample preparation.

The molds were first sprayed with release agent (WD-40) to prevent damage during the removal of samples from the molds. Samples were placed into the molds in two layers. Each layer was compacted by at rubber tamper (dimensions 13 x 25 x 152 mm). After compaction, samples were compacted by 20 drops on a jolting table and vibrated for 30 seconds on a vibrating table (Figure 13).

Figure 13 Vibrating table (left) and Jolting table (right) used for compaction of ECC

After the samples were compacted, the samples were cured in molds for 24 hours at 23˚C and 95% relative humidity. After 24 hours, the samples were demolded and cured in a lime water at 23℃ for 14 days. Prior to testing, specimens were dried at 90℃ for 24 hours.

3.3.2 Mixing procedure for CNF

Even distribution of carbon fibers within the cementitious matrix is important for realizing the proposed concept; improper dispersion has an adverse effect on the strength of the sample and the matrix with inconsistent conductivity. Preliminary tests demonstrated that it was impossible to properly disperse nano fibers in water under ultrasonic treatment. Figure 14 demonstrates the efficiency of the dispersion of CNF in water using an ultrasound mixer and the water for various amounts of time.

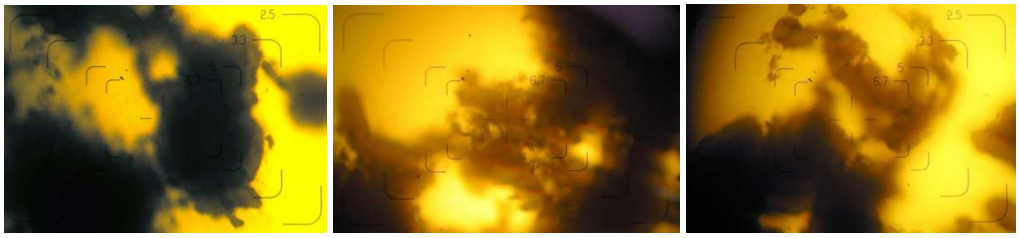

a) b) c)

Figure 14 Clumps of carbon nanofibers in water after ultrasound for: a) 10 min, b) 30 min, and c) 60 min (100x magnification)

Dispersion of the CNFs was achieved by using PCE as surfactant and ultrasound treatment. The superplasticizer was first mixed with water at 2000 rpm for 2 min using a high-speed mixer (Silverson L5M-A). The CNF were added and dispersed using the ultrasound processor (Hielscher UIP1000hd) at 75% of the maximum power (750 W) at 20kHz for 20 minutes. A sample with CNF was dispersed for at 5, 10, 15 and 20 minutes

and analyzed by the optical microscope (Olympus BH-2) at 100x magnification. Figure 15 shows the dispersion of the CNF at various dispersion times.

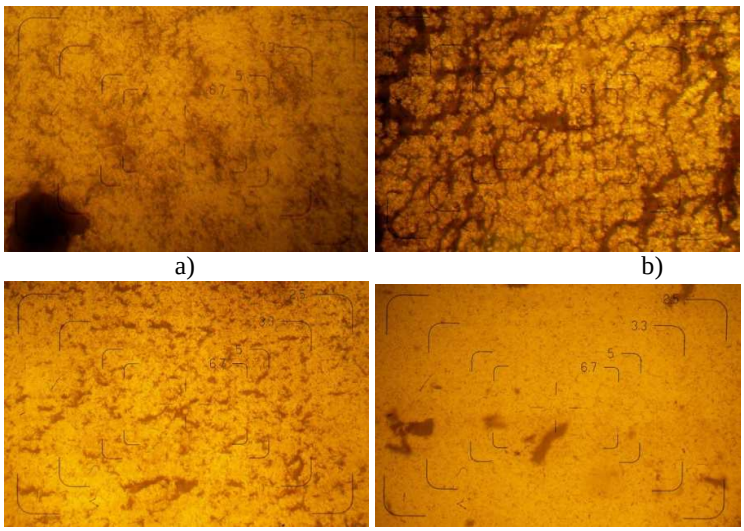

a) b) c) d)

Figure 15 Dispersion of carbon fibers in water using surfactant: ultrasonification for a) 5 min, b) 10 min, b) 15 min, and c) 20 min. (100x magnification)

3.3.3 Mixing procedure for CNT

Production of uniform dispersions CNTs proved to be harder than the CNFs. The same mixing procedure used for the CNFs was attempted with the CNTs, however, after mixing, the CNT remained clumped. The strong attractive forces between surrounding CNTs need to be broken to reduce the agglomeration. This was not possible through the use of PCE and ultrasonification alone. Figure 16 shows the agglomerated fibers and Figure 17 shows the fibers under the optical microscope (Olympus BH-2) at 100x magnification at 5, 10, 15, and 20 minutes of ultrasonic mixing.

Figure 16 Agglomerated CNTs

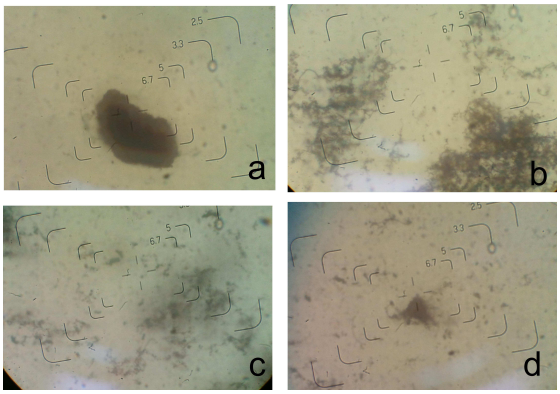

Figure 17 CNTs dispersed by ultrasound a) 5 min b) 10 min c) 15 min d) 20 min

Proper dispersion was achieved through the use of silica sand to the. Silica sand was added to the mixture of PCE and CNTs in the amount of 5% of total sand used before ultrasonification. The quantity of sand added was taken from the total sand in the mix design to help break up the particles to improve the dispersion. The CNT were added and dispersed using the ultrasound processor (Hielscher UIP1000hd) at 90% of the maximum power (900 W) at 20kHz for 20 minutes. A sample with CNT was collected at 5, 10, 15 and 20 minutes and analyzed under the optical microscope (Olympus BH-2) at 100x magnification. Figure 18 shows the fibers under the optical microscope (Olympus BH-2) at 100x magnification at 5, 10, 15, and 20 minutes of ultrasonic mixing.

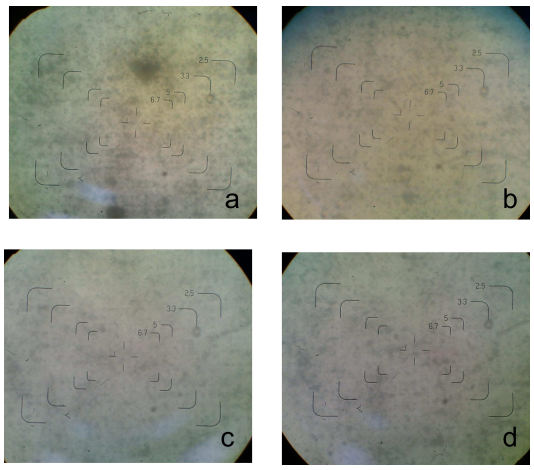

Figure 18 Dispersion of CNTs after the addition of silica sand: ultrasonification for a) 5 min b) 10 min c) 15 min d) 20 min

3.4 Testing of ECC

Specimens were tested to evaluate their mechanical and electrical properties. Evaluations were made both in their fresh and hardened state. The fresh concrete was tested for workability. The hardened concrete was tested to determine the flexural and compressive response as well as the conductivity of the samples.

3.4.1 Flow of fresh mixtures

The workability was tested using a 254 mm (10 inch) flow table (Figure 19) as per ASTM C230 standards.

Figure 19 254 mm (10 inch) flow table

3.4.2 Four point flexural testing

Ordinary portland cement has poor strength when loaded in flexure or in tension. To improve the strength under these loading conditions, PVA and CNT/CNF fibers were used in the mix design. To test the samples for flexural strength, four-point bending test was conducted using a universal testing machine (Instron 3369). The samples used for in this test had the dimensions of 14 x 40 x 160 mm. The top-point loading rollers was placed 40 mm apart, while the bottom loading rollers were spaced at 120 mm. Figure 20 shows the setup of the experiment.

Figure 20 Experimental setup for 4 point bending and electrical measurements

To observe the change in conductivity of the samples and detect cracking, the samples were tested until failure at a loading rate of 1.2 mm per minute. The data acquisition recorded the conductivity of the samples in four second intervals (HP 34970A from Hewlett-Packard).

3.4.2.1 Testing procedures for cyclic loading

Samples were tested for polarization effects before the mechanical testing at each exposure condition. To reduce the effects of the polarization at rest, samples were allowed to depolarize for an additional 30 minutes before the cyclic testing was conducted.

Cyclic testing was conducted on an Instron 3369 compression machine under four point bending. On the tension face of the concrete specimens, rollers were spaced at 120 mm while the rollers on the compression face were spaced 40 mm apart. A load cell with a capacity of 44.5 kN was placed on top of the steel rollers on the compression (top) side to measure the load applied to samples. The steel rollers were covered with electrically

insulating tape to prevent short cuts for the electrical current which would affect accurate readings. To maintain the moisture content in the specimens throughout the duration of the testing, the samples were placed in a sealed plastic bag with a wet cloth to help maintain humidity. This helped to prevent water evaporation from the sample. The set up for the experiment is shown in Figure 20.

After the samples were placed on the Instron machine, they were then hooked up to the data acquisition for resistivity measurements. The data acquisition was turned on and allowed to measure the resistivity for 10 minutes without the influence of mechanical loading. After the initial 10 minutes of monitoring readings, the load was applied for an additional 10 minutes without the influence of externally applied voltage. The samples were loaded in their elastic range to allow for repetitive loading on the samples. To ensure the loading was within the elastic zone, loading was limited to 20% of the maximum load. Loading during cyclic conditions ranged from 10 to 150 N and was applied at a rate of 0.56 kN/min. After the first 20 cycles of testing, the samples were tested again under the same loading conditions, but under external applied voltage. The 9V DC power supply was turned on and the influence was measured by the data acquisition. After the 20 cycles were completed, the sample was allowed to depolarize for 20 minutes and the procedure was repeated twice.

All samples were tested under the cyclic loading conditions regardless of the time of humidity exposure the sample experienced. Samples that were exposed for 24 hours in water were also tested under cyclic loading with 2x of the applied force (300N). The above procedure was repeated after the first loading conditions were applied allowing first for 30 minutes of depolarization. Samples were mechanically loaded from 10 to 300

N for ten cycles. The change in resistivity was measured with and without the application of external voltage following the testing procedure for the first cyclic testing.

3.4.2.2 Failure loading

After testing of the samples under cyclic loading conditions, samples were allowed to depolarize for an additional 30 minutes before being loaded until failure.

Samples were loaded under four point bending until failure using an Instron 3369 compression machine. On the tension face of the concrete specimens, rollers were spaced at 120 mm while the rollers on the compression face were spaced 40 mm apart. A load cell with a capacity of 44.5 kN was placed on top of the steel rollers at the compression (top) side to measure the load applied to samples. The steel rollers were covered with electrically insulating tape to prevent shorts for the electricity to follow which would prevent accurate readings from occurring. To maintain the moisture content in the specimens throughout the duration of the testing procedure, the samples were placed in a sealed plastic bag with a wet cloth to help maintain humidity. This helped to prevent the evaporation of fluids from the sample.

After the samples were placed on the Instron machine, they were then hooked up to the data acquisition for resistivity measurements. The data acquisition was turned on and allowed to measure the resistivity for 10 minutes without the influence of mechanical loading. After the initial 10 minutes of testing, the loading machine was turned on and loaded until failure at a constant rate of 1.2 mm per minute. The data acquisition recorded the conductivity of the samples, as well as stress and strain. Samples were

tested past ultimate loading to test the ability to detect cracking after the initial cracking of samples.

When analyzing the results it was important to ensure the analysis was conducted to eliminate the effect of specimen size dimensions and ensure the easy transition between experimental results and practice. To allow the information gathered to be easily relatable to standard design practices, it was important to use stress and strain conversion that conform to industry standards. The Instron machine used output the data collected in terms of extension and load, so it was necessary to convert the extension and load to strain and stress, respectively using the following equations.

$$\boldsymbol{\sigma} = \frac{6 * P * a}{b * d^2} \quad \textbf{[2]}$$

$$\boldsymbol{\varepsilon} = \frac{3 * \Delta * a * d}{(L - a)^2 * (4 * a - L)} \quad \textbf{[3]}$$

Where:

σ: Stress (MPa)
ε: Strain (mm/mm)
P: the applied load (N)
Δ: the measured deflection (mm)
a: the distance from the end of the sample to the applied load (mm)
d: the depth of the sample (mm)
b: the width of the sample (mm)
L: total length of the specimen (mm)

To collect the resistance readings during the experiments a data acquisition device was used. The equipment used in this work was the HP 34970A from Hewlett-Packard which directly recorded the resistance of the samples. The resistance reading needed to be converted to resistivity and then to conductivity to consider the dimensions of the

individual specimen and location of the electrodes. The following equations were used to convert resistance to resistivity (4) and to conductivity (5).

$$\mathbf{R_s} = \frac{R * h * t}{l} \quad \textbf{[4]}$$

$$\mathbf{C} = \frac{1}{R_s} \quad \textbf{[5]}$$

Where:

R: resistance (ohm)
h: height (mm)
t: thickness (mm)
l: electrode spacing (mm)
R_s: resistivity (Ωm)
C: Conductivity $(\Omega m)^{-1}$

3.4.3 Compressive tests

The compressive strength is often used to judge the performance of a concrete that has been placed in the field. Compressive tests were conducted on both reference samples and CNT/CNF-PVA-FRC to determine the effect fibers. Compressive tests were performed on 50.8 x 50.8 x 50.8 mm cubes in accordance with ASTM C109. The specimens were loaded at a rate of 0.9 kN/sec using an ADR-Auto ELE (Figure 21) compression machine. The maximum load and maximum compressive stress was then recorded.

Figure 21 ADR-Auto ELE compression machine

3.4.4 Tension testing

Through the method proposed for monitoring conductivity in concrete specimens, it was determined that cracks can be detected at four point bending test. Cracks are developed more uniformly under tensile loading when compared to bending, for this reason it was important to load the samples under tension. To test the samples under tension, the preparation method of samples had to be adjusted.

Samples prepared for this type of testing is similar to the sample preparation for the samples tested under four point bending. The samples used for this test had the dimensions of 14 x 40 x 160 mm. A universal testing machine (Instron 3369) loaded the samples under tension at a rate of 0.6 mm/minute under tension. Samples were loaded into the grips that tightened as the load increased. Figure 22 shows the set up for tensile loading of samples.

Figure 22 Experimental setup for tensile testing

This set up allows for the specimens to be loaded under tensile loads only and will allow for samples to experience multiple cracks before failure. The grips used for this type of loading are electrically conductive elements and create an electrical bridge across the element making accurate readings for crack detection impossible. To avoid the electrical short cut, samples were coated in electrically insulating epoxy (Smooth-On MT-13 White epoxy adhesive cement). The epoxy came in two parts and needed to be mixed in equal parts to ensure optimum performance of the materials. The two components of epoxy were batched at equal quantities and mixed thoroughly in a glass container. After mixing, the epoxy was applied to the surface of samples to insulate the rear ends of samples.

The grips used to apply the tensile loads also applied a compressive force to the face of the sample. To help distribute the loads over a larger surface area, the epoxy was applied over the area with the dimensions of 40 x 55 mm (for direct contact with the

grips). It was important to ensure a smooth, uniform surface of epoxy coating allowing for the load transfer from grips of the loading frame without slipping. After the epoxy was applied to the surface of the sample, teflon plates with dimensions of 40 x 55 mm were placed on the specimen. Teflon was used because of its ability to be easily removed from the surface of the sample without bonding to the epoxy coating. After the Teflon and epoxy were placed, a piece of plastic was placed over the sample and a 20 pound weight was placed on the samples to apply constant pressure to the surface of the sample. The epoxy was allowed to harden for 24 hours before the weight and the plates were removed from the samples. Each face of the specimen that came in contact with grips while loaded in tension was covered with epoxy to ensure complete the insulation. Figure 23 shows the samples with the epoxy coating.

Figure 23 Epoxy coated zones of samples

Predicting the location of crack formation in samples loaded under tension presented a challenge. In preliminary tests many samples tested in tension had cracks form near the grips, which were outside of the electrode range, therefore, it was necessary to ensure the samples cracked between the electrodes. Stress concentrators were introduced into the samples to ensure the crack formation occurred between the electrodes. To create the stress concentrations, cuts were made in the samples on either side of the sample at the midpoint. The cuts had dimensions of 5 x 5 mm for initial

testing. The cuts in the samples were made after the electrodes were attached to the surface of the samples extra care was taken to ensure the integrity of the electrodes was not compromised. Figure 24 demonstrates the samples prepared for testing.

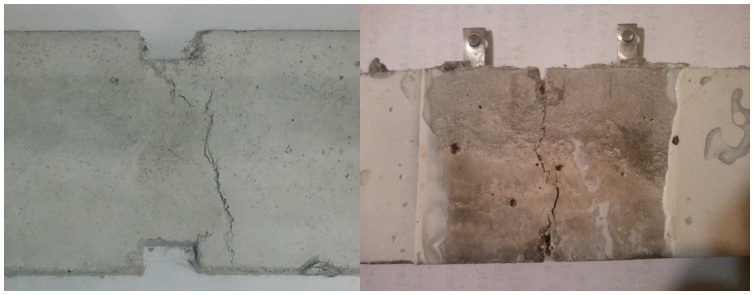

Figure 24 Prepared samples for tensile testing initial (left) and final (right)

Monitoring the change in conductivity to determine crack formation was an essential part of this experiment. When using the four point bending test, it was necessary have multiple locations for electrodes along the side loaded in tension. The grips, as stated before, act as an electrical bridge and do not allow for the electrodes to be placed in these areas. Two channels of the external electrodes were placed on either side of the sample located at 20 mm (channel 1) and at 40 mm (channel 2). Figure 25 shows the external electrode placement for samples loaded for tensile testing.

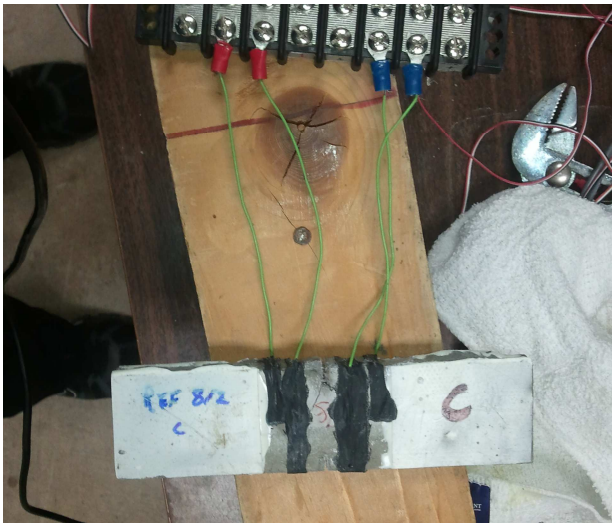

Figure 25 External electrode placement

3.5 Electrodes

The specimens were prepared for two- and four-probe electrical resistance measurements. For the reported experiment the two-probe DC testing method was chosen because of the simpler instrumentation and ease of implementation in the field [27, 46]. The electrical resistance data were directly measured for particular channel and recorded using data acquisition (HP 34970A from Hewlett-Packard).

3.5.1 External electrodes

The external electrodes were added to the samples after they had been allowed to cure. The electrical contacts were glued using "Wire Glue" (Anders Products) to the surface of the specimen on both the tension and compression sides. A coating of latex (Daraweld, from WR Grace) and rubber mastic were placed over the dried glue to make the waterproof connection. The electrodes were attached to the samples in pairs (Figure 26). Three pairs of the electrodes were attached on the tension side of the specimen,

while the fourth set (Channel 1) was placed on the top of sample in the compression zone. The electrodes were attached in pairs to investigate the electrical drop over the distance between the electrodes. The power supply electrodes were placed on the tension side of the sample 140 mm apart. The Channel 2 and 3 electrodes were placed 40 mm and 120 mm apart on the tension side, respectively. The Channel 1 electrodes were placed 20 mm apart on the compression side of the sample (Figure 26). In this research, external power was not applied, and the two-probe method was used; the resistance was measured directly by data acquisition (Channel 1 measurements are not reported).

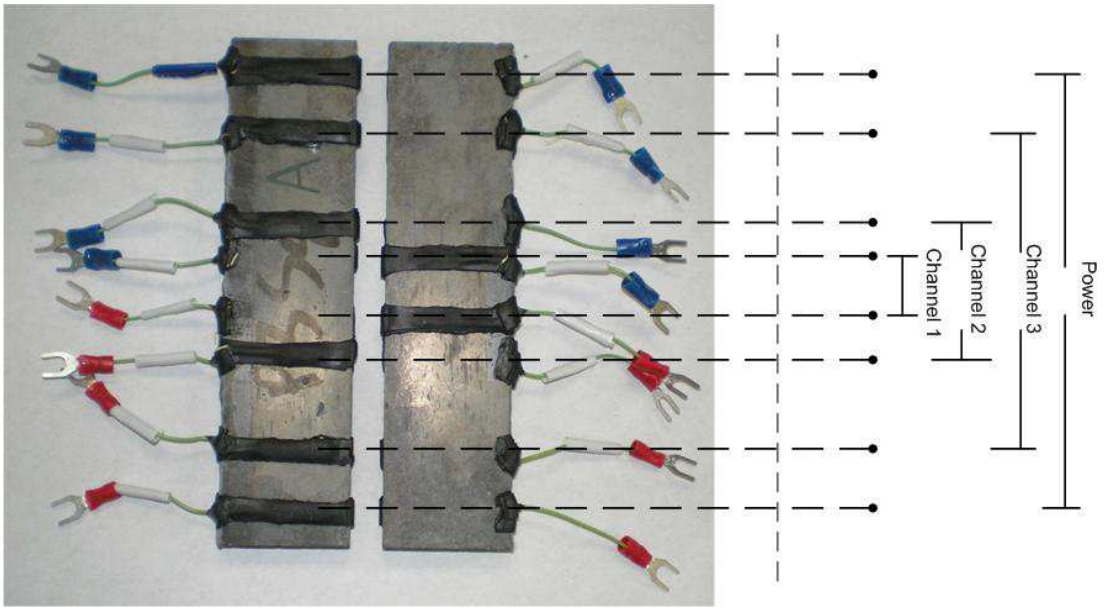

Figure 26 Electrode placement and channel coding

3.5.2 Embedded electrodes

External sensors have the issue of being exposed to the environment due to a lack of concrete cover. Embedded sensors are placed in the forms before the concrete is placed and cannot be altered. The sensors for this work are 26 gage stainless steel cut to

the dimensions of 5 x 100 mm. The steel is bent at a 90° angle between 44 and 50 mm from each end (Figure 27). This creates a U-shape that allows for one end to stick out the top of the sample and the other end to remain embedded in the sample. The extruding electrode was used for the connection to the data acquisition and of electrical resistivity.

Figure 27 Design of stainless steel electrodes: Unbent (bottom) and Bent (top)

Embedded sensors must be placed securely in the mold to ensure that the sensors have not moved during the placement of the concrete. To control the placement, the embedded sensors were attached to a fiberglass mesh (supplied by a local distributer) and placed in the mold. To ensure proper concrete cover, the height of the mesh was limited to 36 mm and to allow for the mesh to cover all sides of the sample the length of the mesh was cut to 350 mm. Mesh was stretched to keep the mesh in position and electrodes in the correct locations. This was done by placing 40 mm plastic tubes on the ends of the mold and wrapping the mesh around the tubes allowing 40 mm of overlap. Electrodes were attached into the mesh to ensure proper locations. Four electrodes were placed in the concrete at 20 mm and 60 mm from either end of the sample. Figure 28 shows the mesh and location of electrodes.

Figure 28 Embedded electrodes assembly

3.6 Resistivity measurements

Polarization is an important parameter to consider when DC is used to probe the self-sensing materials. Polarization interferes with resistivity measurements [40,46], and it continues to grow over the time of measurement until it reaches a plateau, at which the readings can be attributed to "saturated" conditions and used as an indication of the stresses experienced by the sensor. The piezioresistivity and conductivity of PVA-FRC materials change in proportion to strain. The resistivity was measured by the data acquisition after each level of moisture exposure without the influence of mechanical loading. To eliminate the influence on conductivity measurements, samples were placed on an electrically insulating material. Resistivity readings were monitored by the data acquisition that was connected through a series of electrodes attached to the specimens (Figure 29).

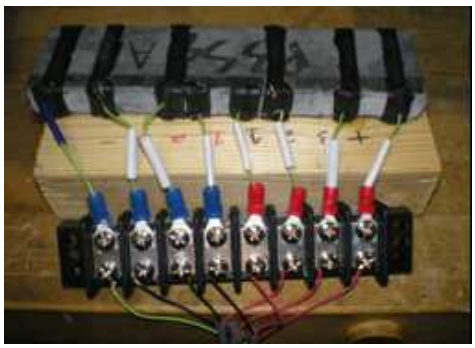

Figure 29 Set up for monitoring sample resistivity

The data acquisition was turned on and allowed to measure the resistivity for a ten minute period. After the initial readings were conducted, the 9V DC power supply was switched on and the resistivity of the material under external current was recorded for an additional ten minutes. At the end of this stage, the data acquisition and power supply were disconnected and samples were allowed to depolarize for 20 minutes. After the rest period, the samples were tested an additional two times following the same procedure.

Samples exposed to moisture experience a change in conductivity. Dry samples have higher resistivity than those exposed to moisture. Increased conductivity in samples was achieved while exposing samples to different moisture conditions due to the conductive nature of the water and Na chloride mixtures. The moisture conditions did not prevent the polarization effects in the samples from occurring and, therefore, need to be analyzed to consider these effects.

3.6.1 Change in conductivity

Materials exhibit electrical characteristics based on their dimensions and physical properties. Changes to the physical structure of the materials change the overall conductivity. Concrete does not conduct electrical current, however, it is not completely insulating. Monitoring the change in electrical conductivity due to air void formation through the developments of cracks under loading can lead to crack detection. Direct readings of conductivity are not ideal due to polarization experienced by concrete due to the applied electrical current. Two methods for analyzing the raw data of conductivity gathered by the data acquisition are proposed.

The piezioresistivity and conductivity of PVA-FRC materials change in proportion to strain and so the proposed relative conductivity method allowed for crack detection of FRC. When comparing the data for the relative conductivity C/C_0 with the stress-strain curve, the strong correlation between the cracking of the FRC and the relative change in conductivity can be observed.

The relative conductivity is defined as:

$$\Delta C / C_0 = \frac{C_t - C_0}{C_0} \quad \textbf{[6]}$$

Where

ΔC- change in conductivity, $(\Omega m)^{-1}$
C_0 - initial conductivity, $(\Omega m)^{-1}$
C_t - conductivity at a testing time t, $(\Omega m)^{-1}$

The differential change conductivity can be defined as:

$$\Delta C_t / C_t = \frac{C_t - C_{t-\Delta s}}{C_t} \quad \textbf{[7]}$$

Where:

C_t - conductivity value at a testing time t, $(\Omega m)^{-1}$
$C_{t-\Delta s}$ - conductivity at a testing time t- Δs , $(\Omega m)^{-1}$
ΔC_t - change in conductivity at sampling rate Δs, $(\Omega m)^{-1}$
Δs – Sampling rate

3.7 Exposure to moisture/Na chloride solutions

Before testing, samples were immersed in water or 2% Na chloride solution for 24 hours to simulate the effect of different exposure conditions. The absorption of water and Na chloride solution for reference PVA-FRC 3.8 and 4.0% respectively. Specimens of CNF-PVA-FRC had slightly higher 24 hour absorption 3.7 and 3.7% for water and

chloride solution, respectively. The stress-strain and electrical resistance of the reference PVA-fiber composite specimens was compared with CNF-PVA fiber composite; one group of specimens was exposed to water while the other was exposed to chloride (2%) water. The two exposures allowed investigation of the sensitivity of composite to detect the presence of chlorides; therefore, the reported experiment was designed to observe the change in relative conductivity of CNF-based specimens under flexural conditions.

Table 7 Experimental Plan

	Exposure type	
Specimen type	Water 24h	2% NaCl2 24h
Reference PVA-FRC	+	+
CNF-PVA-FRC	+	+
CNT-PVA-FRC	+	+

The procedure used in the initial study for exposing the samples to moisture conditions was adjusted to meet ASTM testing requirements. The procedure in ASTM C1202-09 was referenced when determining the following procedure. The ASTM procedure requires that all the tested materials be subjected to a vacuum (at a pressure of 30 in Hg) for 3 hours before coming in contact with de-aerated water.

It was important that samples are saturated in de-aerated conditions described by the ASTM. To de-aerate the specimens, tap water was allowed to boil and cool to ambient temperatures in a sealed container before coming into contact with the samples. Once the water was prepared, it was placed in a container attached to the air tight container containing the prepared samples. To remove all the air trapped in the pores of the samples, the samples were placed under a vacuum to a pressure of 30 in Hg for 3 hours. After 3 hours, water was allowed to enter the chamber under the applied pressure

for an additional hour. After the hour had lapsed, the pressure was removed from the chamber and the samples remained submerged for an additional 18 hours. After the procedure was completed, samples were tested to determine the effect of moisture conditions on the conductivity of concrete samples. Figure 30 displays the set up for described procedure.

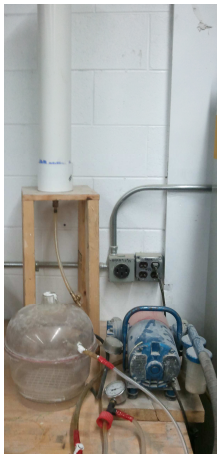

Figure 30 Chamber set up of vacuum

4 Preliminary Research Results

To determine the parameters of the study an initial experiment was conducted. The initial study was used to determine specimen preparation methods as well as loading styles and various other conditions. The parameters of the study include; PVA fiber and superplasticizer content, mixing procedures, mesh preparation, exposure time to water and Na chlorides, loading of the samples, and resistance measurement and analysis.

4.1 Exposure time

Conductivity is affected by moisture. Pure water is a poor conductor of electricity; however, interpore water in portland cement concrete/composite is saturated with $Ca(OH)_2$ and often alkalis. Furthermore, water that the concrete structures are exposed may have different contaminants. Water in the environment may contain metal ions and other contaminants that allow it to conduct electric current. One pollutant that is common on roadways is sodium chloride originating from deicing salt. Water that contains dissolved sodium chloride has a higher conductivity. When salts dissolve in water, they break into the ions, allowing for electricity to be easily conducted over this medium.

There are many other pollutants that occur naturally in our environment that may affect the electrical conductivity of water. This work focused only on chlorides in water due to the commonality of these ions in roadway projects. Deicing salts do not directly affect the concrete, but corrode the reinforcing steel. When steel corrodes, it undergoes a volume expansion which leads to an increase in internal stresses in the concrete and causes local and global failures in the structure. For this reason, the progression of Na

chlorides into the concrete is an important parameter governing the service life of reinforced concrete structures.

Samples were tested mechanically under different levels of exposure to water and Na chloride solutions. In the study, samples were tested at two exposure times that included the 0 and 24 hours. Samples were exposed either tap water or a 2% sodium chloride (NaCl) solution by mass of tap water. To understand how conductivity in the specimens were effected by moisture exposure, the samples were monitored without mechanical loading for 3 minutes.

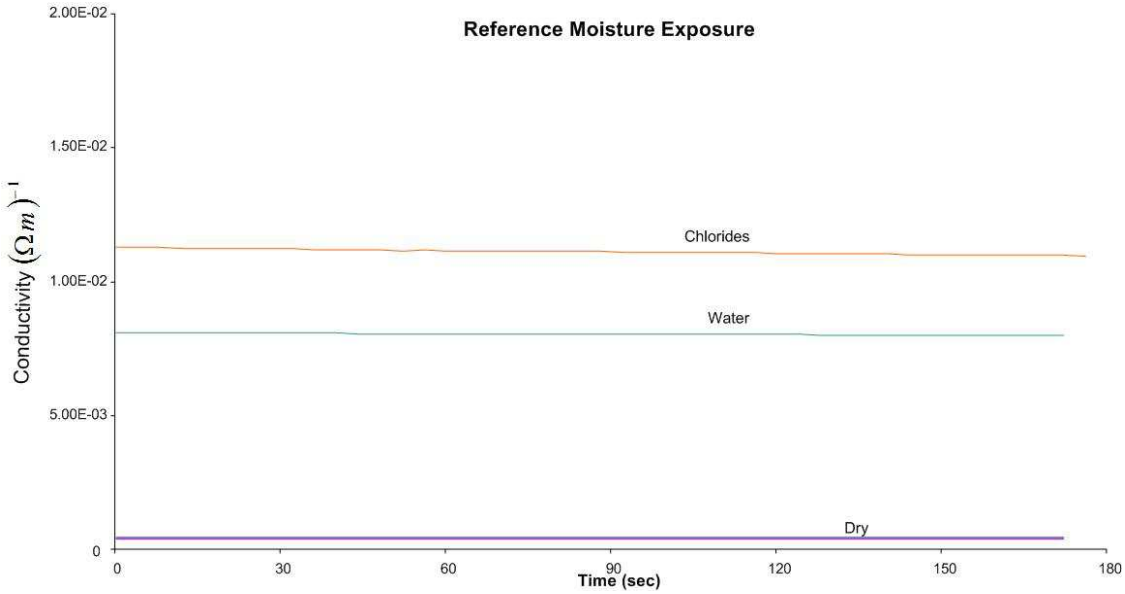

Figure 31 The conductivity of Reference-PVA-FRC samples with various moisture exposures (channel 2).

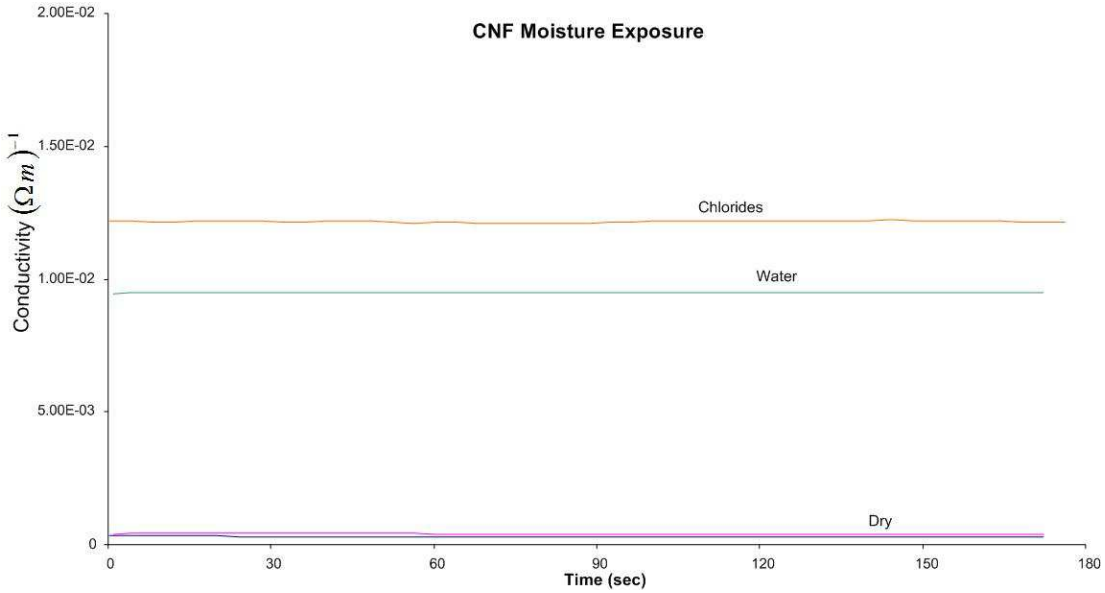

Figure 32 The conductivity of CNF-PVA-FRC samples with various moisture exposures (channel 2).

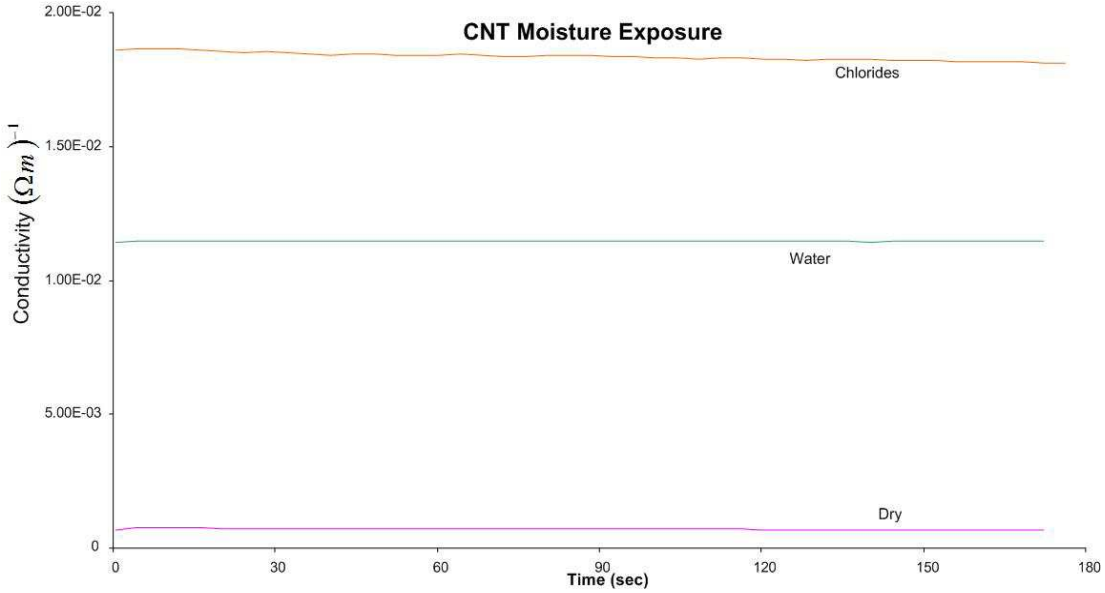

Figure 33 The conductivity of CNT-PVA-FRC samples with various moisture exposures (channel 2).

Figure 31, Figure 32, and Figure 33 demonstrate the change in measured conductivity for samples exposed to different moisture conditions for a given time period. In these figures, the samples were not mechanically loaded which allowed for the effects

of moisture on the samples to be monitored directly. The three mix designs considered were monitored for conductivity at plotted against time after the given exposure time. When samples were exposed to water or Na chloride solutions, the corresponding conductivity, depending on the exposure time, increased significantly. Dry samples had the lowest measured conductivity while conductivity in samples that were exposed for 24 hours increased by $7.64x10^{-03}\Omega^{-1}m^{-1}$ and $1.07x10^{-02}$ for reference-PVA-FRC samples exposed to water and Na chlorides respectively. The increase in conductivity correlates to a decrease in resistivity in samples. Table 8 displays the conductivity of samples tested under given moisture conditions.

Table 8 Effect of moisture conditions on conductivity

	Conductivity ($\Omega^{-1}m^{-1}$)		
	Reference-PVA-FRC	CNF-PVA-FRC	CNT-PVA-FRC
Dry	$4.13x10^{-04}$	$4.20x10^{-04}$	$7.25x10^{-04}$
Water	$8.06x10^{-03}$	$9.49x10^{-03}$	$1.15x10^{-02}$
Na Chlorides	$1.12x10^{-02}$	$1.22x10^{-02}$	$1.84x10^{-02}$

4.2 Current- voltage characteristics

The effect of water and NaCl exposure on current voltage characteristics of FRCs was investigated. It can be observed that all tested FRC had an almost linear response within the tested range from -15 to 15V. It can be concluded that the conductivity of dry CNF-PVA-FRC is slightly higher than that of reference material, $4.20x10^{-04}\Omega^{-1}m^{-1}$ vs. $4.13x10^{-04}\Omega^{-1}m^{-1}$, respectively. 24 hour exposure to water of investigated FRC resulted in significant increase in conductivity to $9.49x10^{-03}\Omega^{-1}m^{-1}$ vs. $8.06x10^{-03}\Omega^{-1}m^{-1}$, respectively. Surprisingly, the type of exposure (i.e. presence of chlorides) had a little

effect on conductivity (Figure 34), probably to very dense cementitious matrix and difficulties for chloride ions to penetrate the entire specimen.

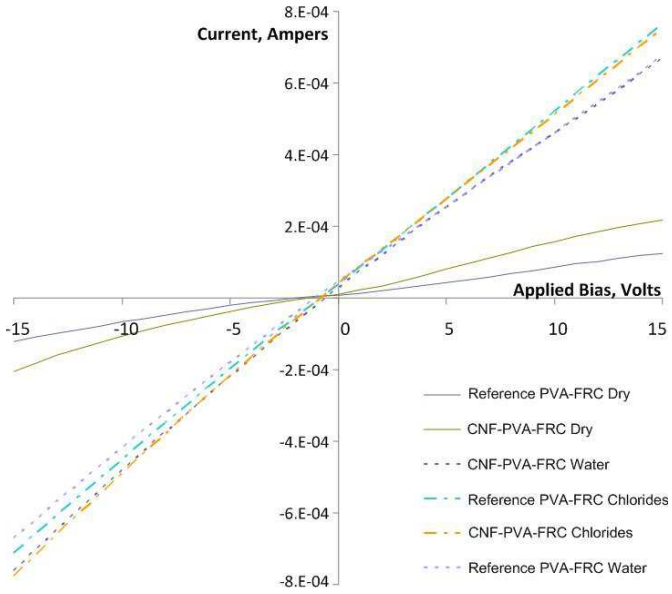

Figure 34 Current-Voltage characteristics of investigated FRCs (Channel 2).

4.3 Cyclic loading

Using the relative analysis for analyzing the conductivity data this method demonstrated the ability of CNF-PVA-FRC to act as a stress sensor. In Figure 36 and Figure 37 the change in conductivity was due to mechanical loading on the samples. The cycles are clearly defined and follow the loading pattern shown in Figure 35. Due to the lack of negative loading, the stresses in the samples accumulated and the samples did not return to their original, undeformed shape which caused the strain to increase from cycle to cycle in both loading cases. Also, due to polarization, the conductivity was shown to decrease over time. Polarization effects on samples are displayed in Figure 56 to Figure 61 in the appendix. Through the conductivity measurements, it was shown that detecting the loading response of samples was possible. Allowing for the detection of loading is

useful for monitoring traffic volumes as well as gives the possibility to detect and monitor the weight of vehicles on bridges or roadways. Since samples were only measured in their elastic zone, crack formation was not observed in these tests.

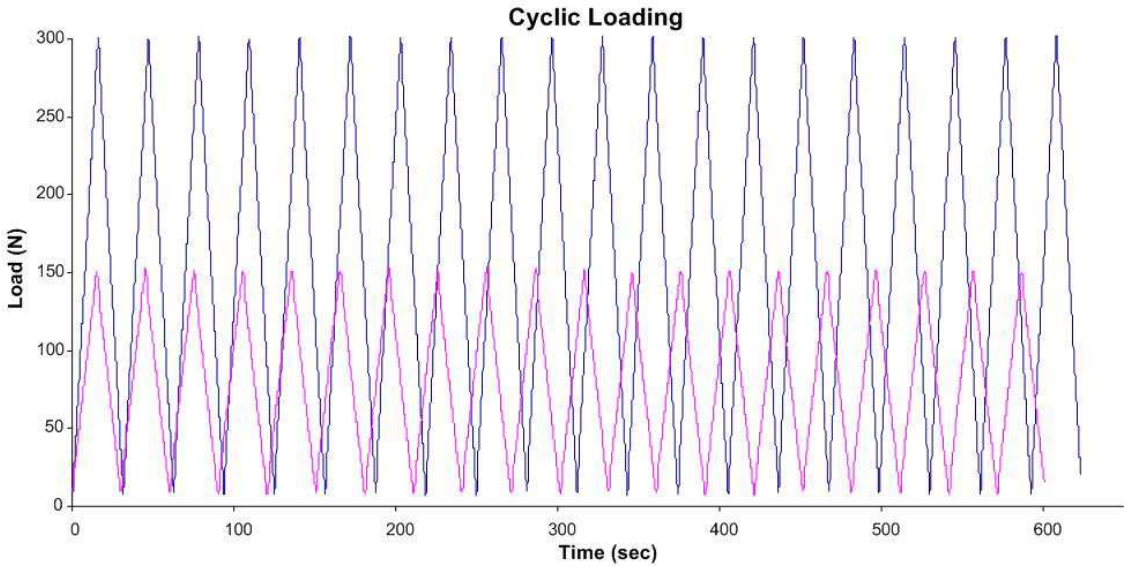

Figure 35 Cyclic loading pattern

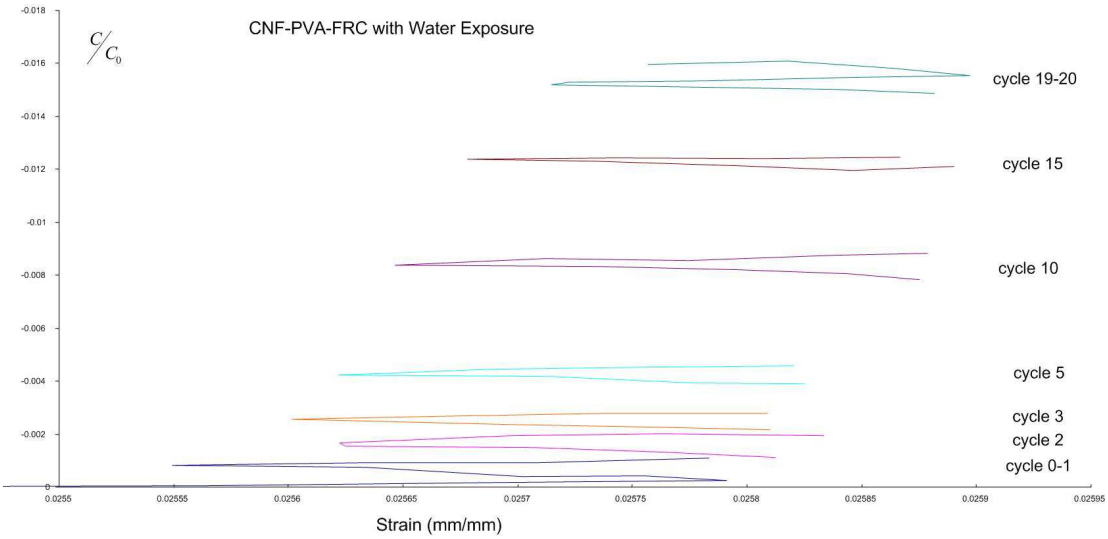

Figure 36 Conductivity of CNF-ECC samples (reverse scale channel 2) under cyclic loading (150N)

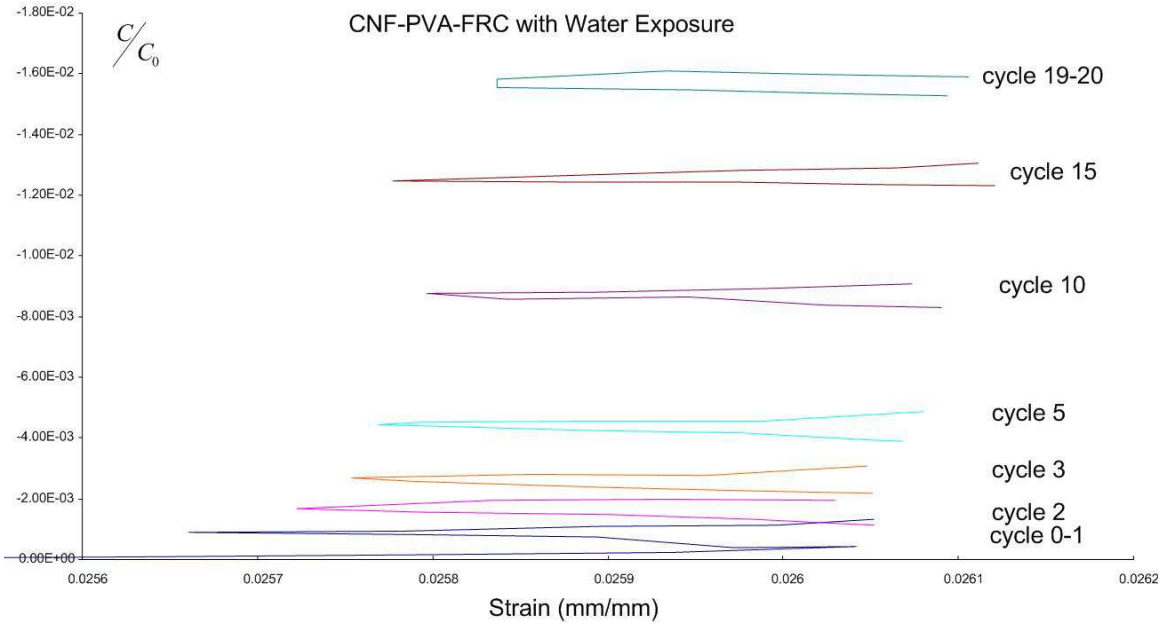

Figure 37 Conductivity of CNF-ECC samples (reverse scale channel 2) under cyclic loading (300N)

4.4 Test results: flexural loading

In the four point bending test, the conductivity response of FRP changes its slope after a first major crack at a strain of 0.0019 mm/mm (Figure 38). A similar response was demonstrated by the CNF-PVA based FRC (Figure 39). Before the samples cracked, the conductivity response had a relatively low, but distinctive slope; after first crack the slope of relative conductivity was drastically changed, indicating post-cracking response (dependent to electrode spacing).

The differential conductivity method for data analysis allowed for crack detection as shown in Figure 38 and Figure 39 for reference FRC and CNF-PVA-FRC, respectively. When comparing the data for the fractional change in conductivity with the stress-strain curve, there is a match between the specimen cracking and the fractional change in conductivity. When the first major crack appears in the reference FRC at a strain of 0.0019 mm/mm, the differential conductivity has a spike at the same strain

(Figure 38). Cracks are voids in the concrete matrix and act as electrical insulators decreasing conductivity [15]. The strong spike in the reference sample for the initial crack is more defined than the following cracks experienced by the sample at 0.0036 and 0.0044 mm/mm (Figure 38), because of progressively reduced conductivity of the PVA-FRC composite. There are less-defined spikes in conductivity at larger strains that correlate with the formation of multiple cracks.

Figure 39 shows the performance-electrical response of CNF-PVA-FRC material. The CNFs were used to increase the self-sensing ability of the cement matrix. The relative conductivity was observed to decrease with stress at a very low rate until the first crack formed at a strain of 0.0018 mm/mm (Figure 39). After the first crack, there is a significant change in relative conductivity rate correlated with the response of cracked matrix. The following major cracks at strains of 0.0021 and 0.0024 mm/mm (Figure 39) are better defined compared with the reference FRC, which is probably due to the carbon fibers bridging the cracks in the concrete, lowering the defect sizes and increasing the local conductivity of samples.

The change in differential conductivity of FRC due to cracking was more definite in specimens containing CNF. The smaller changes in conductivity of CNF-PVA-FRC after the main cracking could be attributed to micro-cracking. The smaller cracks led to a smaller change in conductivity and were less defined than the major cracks. These changes are important for detecting micro-cracks and, therefore, nondestructive monitoring of structures. There also appeared to be a correlation between the change in conductivity and chloride ingress. When comparing the differential conductivity method in Figure 39a and Figure 39b there is a larger fractional change in conductivity when

chlorides are present. Samples with sodium chloride exposure has higher conductive capabilities and because of these properties, at the crack occurrence, the change in conductivity is larger, causing the difference to be monitored. Figure 38a and Figure 38b also demonstrate this ability, however, it is much less defined than samples containing CNFs.

There are distinct differences in conductivity for the two channels used in this work. Channel two had the higher changes in conductivity experience for both the relative and differential methods of conductivity analysis defined by equations 6 and 7, respectively. The conductivity could be affected due to crack formation and added stresses. When samples are loaded under four point bending, cracks first appear at the area of highest moment. In this work, the cracks were bridged by either PVA fibers or a combination of PVA/CNF fibers that had large tensile strength causing the sample to crack again in another location instead of propagating. The introduction of multiple cracking caused the conductivity, over the longer span, to decrease due to the higher number of void spaces. The conductivity of the samples was also lower in channel 3 because of the longer distance the electrons had to travel. The energy used to transport the electrons over the medium would be lost to heat due to the resistance of the concrete. The longer span between the electrodes is more area for the electrons to travel which leads to a loss in conductivity for channel 3.

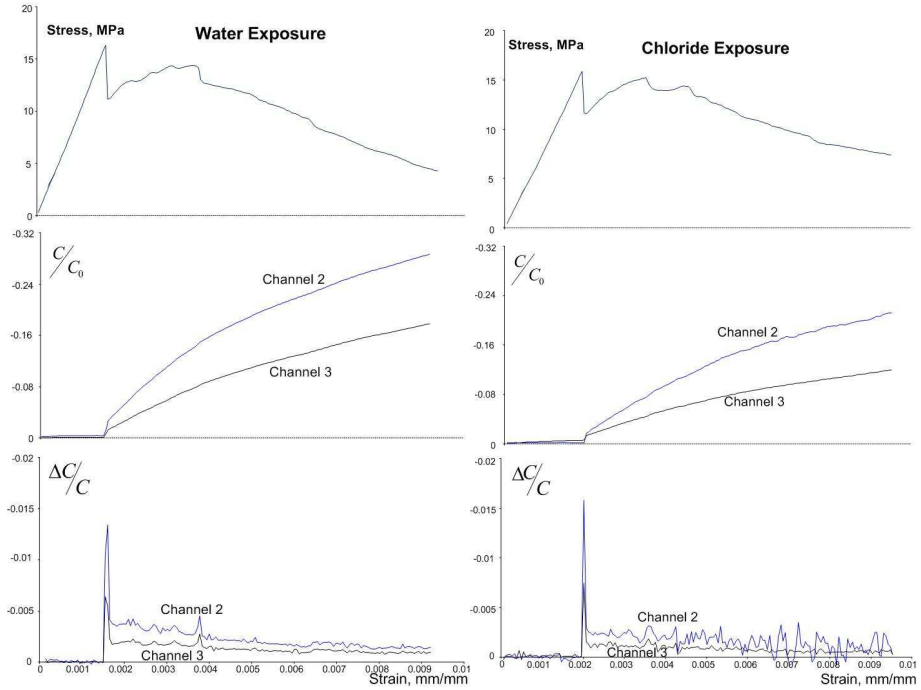

a) b)

Figure 38 The stress-strain performance and relative conductivity (reversed scale) of reference FRC/ECC: after 24h exposure to a) tap water; and b) 2% Na chloride solution

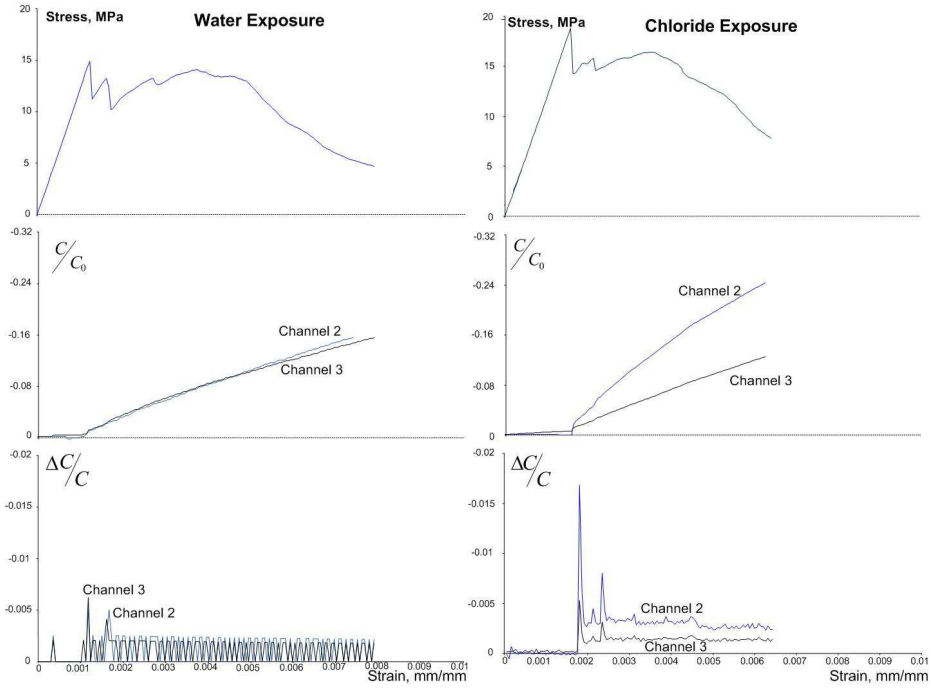

a) b)

Figure 39 The stress-strain performance and relative conductivity (reversed scale) of CNF-PVA based FRC/ECC after 24h exposure to: a) tap water and b) 2% NaCl solution

4.5 Test results: tensile loading

Samples were loaded under tension to verify that the proposed method of crack detection would provide valid results under pure tension. For the initial testing, plain PVA-FRC samples with external electrodes were tested. Samples tested were submersed in water for 24 hours before being loaded until failure. Plain samples, samples without CNFs/CNTs, proved to have self sensing abilities under this loading condition. When the sample experienced initial cracking, the samples experienced a large change in conductivity indicating crack formation. At the loading rate used and due to crack inducing precut, only the crack that lead to total failure was observed (Figure 40). This

work is interested in detecting the multiple cracks that, therefore, the loading rate was reduced to 0.56 mm/minute to allow for better crack detection.

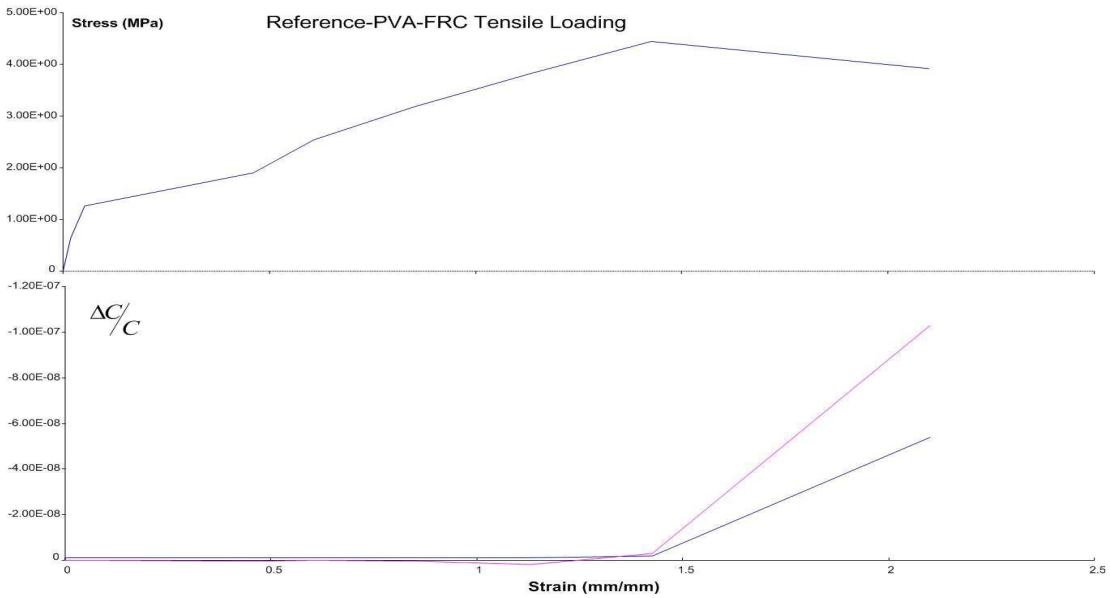

Figure 40 Reference-PVA-FRC under tensile loading (rate 1.2mm/minute)

5 Main Research Results

5.1 Mechanical properties

To improve the tensile properties of the concrete specimens tested, PVA, CNF, and CNT materials were added to the mix design. In addition to the improved mechanical properties of samples, the addition of fibers to the matrix creates a denser, less permeable concrete. In this work PVA, CNT, and CNF fibers were added in different proportions to the mortar mix to determine how these fibers affect the strength under various loading conditions. The various loading conditions considered were 4 point bending, tensile, and compressive loading. The composition of the samples tested is listed in the Table 9.

Table 9 Mixture proportions of investigated CNF/CNT/FRC.

Composition	Reference FRC	CNF PVA-FRC	CNT PVA-FRC
W/C	0.3	0.3	0.3
S/C	0.5	0.5	0.5
SP, % w cement	0.175	0.175	0.236
PVA fibers, % vol	2	2	2
Carbon nanofibers, %vol	0	0.2	0
Carbon nanotubes, %vol	0	0	0.2

5.1.1 Compressive strength

Compressive strength of concrete is in an important property for construction purposes. Most construction projects require that the material placed meets a minimum compressive strength before construction can continue. For this reason, it is important that the admixtures in the mix design have limited the effects on compressive strength at all stages of cement hydration. The three mix designs used in this work were tested under compression to determine the effects of carbon nanotubes/nanofibers to the mix on the overall compressive strength. Compressive strength testing was conducted at the age of 1, 7, and 28 days after the samples were cast. The results of the tests are summarized in Table 10 and graphically in Figure 41.

Table 10 Compressive Strength of Specimens

	Compressive Strength (MPa)		
Sample	1 Day	7 Day	28 Days
Reference-PVA-FRC	37.28	69.05	91.57
CNF-PVA-FRC	36.91	83.62	82.29
CNT-PVA-FRC	32.07	61.88	81.11

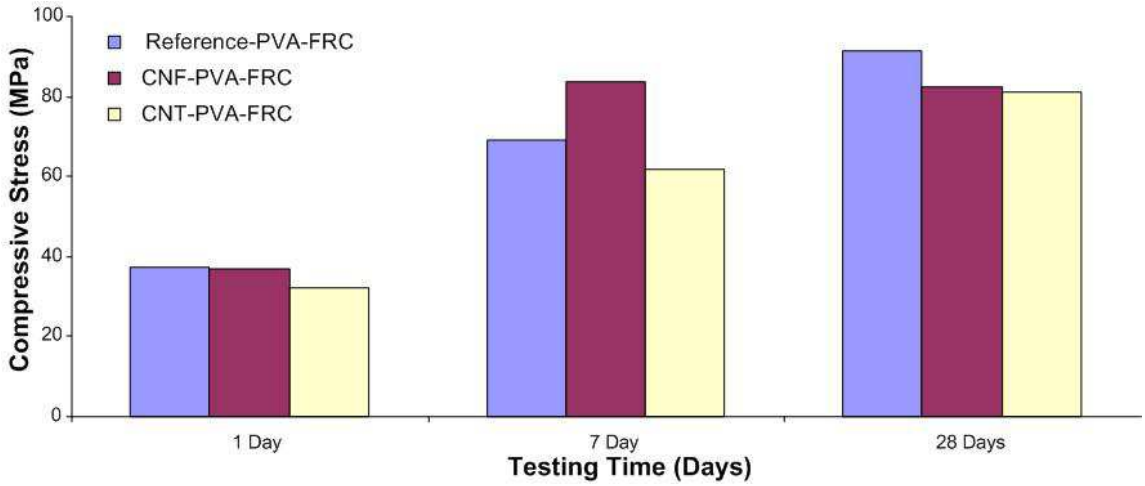

Figure 41 Compressive strength of specimens

The addition of CNT and CNF into the FRC reduced the performance of the material under compressive loading. The reference material performed better under compressive loading than the samples with CNT or CNF for all the time periods observed excluding the CNF-PVA-FRC at a time of 7 days. There was a loss of compressive strength observed for all samples containing carbon nanofibers or carbon nanotubes at the age of 1 and 28 days. Samples containing CNTs had a loss of 14% and 11% for 1 and 28 days age, respectively while the samples containing CNFs had a loss of 1% and 10% for 1 and 28 days age, respectively when compared to the reference samples. At the 7 day age, samples containing CNF had a 21% increase in compressive strength when compared to reference materials, while samples containing CNT had a 10% reduction in compressive strength.

The addition of carbon fibers to FRC in this work reduced the compressive strength; carbon nanotubes and carbon nanofibers can decrease the porosity of the samples by filling the voids that are created during cement hydration; however, the tested samples do not contribute to the compressive capacity of the samples possibly due to imperfect mixing. The CNFs and CNTs used have high tensile properties having failure modes through fiber pullout instead of breaking of the fiber due to their high tensile capacities [8]; however, do not contribute to the compressive strength of the material.

5.1.2 Flexural strength

Concrete is often used as girders in bridge designs or in the structural floor systems of buildings. These elements often span long distances without bracing causing large stresses to occur at the midspan of the member. Concrete has a smaller capacity for

the tensile stresses experienced at these locations and must be reinforced to provide sufficient capacity at these areas. Due to the low capacity in these regions, concrete members often form flexural cracks under low loading causing the steel reinforcement to be exposed and increase the risk of degradation of the flexural reinforcement. These areas are often the most critical to observe for inspectors on projects. To determine the flexural capacity of the mix designs used, samples were tested under four point bending. Testing was conducted using a universal testing machine (Instron 3369) at a loading rate of 1.2 mm/minute following the procedure in section 3.4.2. The maximum flexural stresses achieved are summarized in Table 11 and Figure 42.

Table 11 Flexural Strength of Specimens

	Flexural Strength (MPa)	
Sample	Without fiberglass mesh	With fiberglass mesh
Reference-PVA-FRC	13.33	18.60
CNF-PVA-FRC	10.54	19.39
CNT-PVA-FRC	12.45	14.19

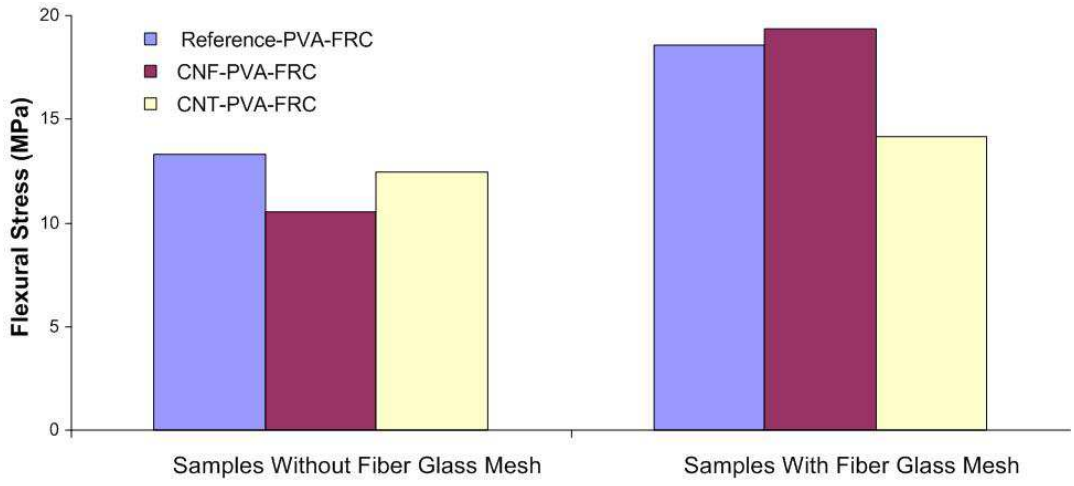

Figure 42 Flexural strength of specimens

Reference specimens containing only PVA fibers had the highest flexural capacity. Due to the high tensile capacity of the CNFs and CNTs, the reduction in flexural capacity was unexpected. The reduction in this capacity is probably due to an unequal distribution of the CNF/CNT in the mortar matrix and excessive air entrainment. Without proper alignment of the CNTs and CNFs, these materials may not have been able to contribute the strength of the system as expected.

5.1.3 Tensile strength

Tensile testing of samples was conducted to determine the capacity of the material under these loading conditions. Testing of samples was conducted using a universal testing machine (Instron 3369) at a loading rate of 0.6 mm/minute following the procedure in 3.4.4. A slower loading rate was used in order to initiate multiple cracking points before failure due to the abrupt failure of concrete due to its brittle behavior. To create a localized stress concentration at the middle of the specimen, the cuts at the top and bottom of the sample with dimensions of 1 x 5 mm was made. This allowed for the specimen to fail between the electrodes, so the conductivity characteristics of the specimen could be observed. The maximum tensile stresses achieved are summarized in Table 12 and Figure 43.

Table 12 Tensile Strength of Specimens

	Tensile Strength (MPa)	
Sample	Without fiberglass mesh	With fiberglass mesh
Reference-PVA-FRC	4.14	6.53
CNF-PVA-FRC	4.27	5.27
CNT-PVA-FRC	4.09	5.86

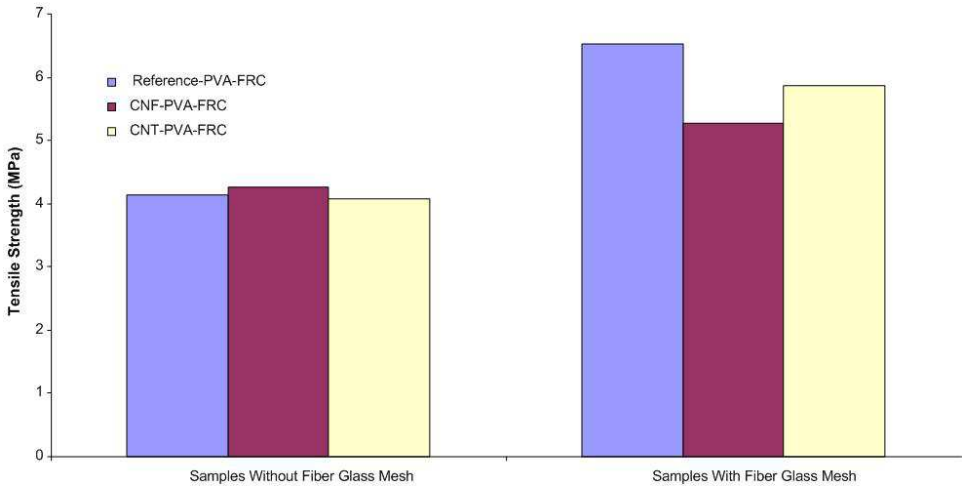

Figure 43 Tensile strength of specimens

As with flexural capacity of specimens containing only PVA fibers had the highest tensile capacity. The properties of the CNFs and CNTs would lead to the conclusion that the inclusion of these materials to the mix would increase the tensile capacity of a specimen. The decrease in tensile capacity could be linked to improper dispersion of CNFs and CNTs and excessive air entrainment into to the mortar matrix.

5.2 Conductivity study

Concrete has a natural ability to conduct electricity. The ability of the material to conduct electricity, however, is dependent on moisture content of the concrete. To increase the ability of the concrete to conduct electricity, CNTs and CNFs were added to the mix design. Using the data acquisition (HP 34970A from Hewlett-Packard) the resistance of the concrete was measured for three conditions: dry, 24h exposure to water, and 24h exposure 2% to NaCl solution. Measurements were made across two channels of electrodes and the averages are displayed in Table 13.

Table 13 Conductivity of Samples

	Conductivity $\Omega^{-1}m^{-1}$					
	Channel 1			Channel 2		
Sample	Dry	Water exposure	NaCl Exposure	Dry	Water exposure	NaCl Exposure
Reference-PVA-FRC	7.42E-04	7.60E-03	7.21E-03	7.35E-04	9.47E-03	1.45E-02
CNF-PVA-FRC	6.42E-04	8.86E-03	1.15E-02	6.66E-04	1.11E-02	1.84E-02
CNT-PVA-FRC	1.39E-03	8.66E-03	1.16E-02	7.92E-04	1.12E-02	1.58E-02

5.2.1 Effects of carbon nano fibers/nanotubes on conductivity

Observing the effects of adding CNFs and CNTs is most evident in the dry state. When comparing dry samples, only the materials natural ability to conduct electricity is observed. All of the samples tested were able to conduct electricity; however, the samples that contained CNT conducted electricity more efficiently.

The CNFs/CNTs used in this work increased the conductivity of the material by reducing the materials resistivity, especially for CNT-PVA-FRC. The conductivity of the dry material increased by 1.87% and 1.08% for Channels 1 and 2 respectively when compared to the Reference-PVA-FRC. Table 13 summarizes the electrical conductivity of samples.

5.2.2 Effect of moisture exposure

After exposing the samples to the intended moisture conditions, it was necessary to test the absorption of the samples. Table 14 displays the average water absorption for the samples.

Table 14 Average absorption

	Moisture absorption (%)	
Sample	Water	Na Chlorides
Reference-PVA-FRC	1.30	1.57
CNF-PVA-FRC	2.98	2.74
CNT-PVA-FRC	2.83	3.40

The samples tested absorbed similar amounts of water when comparing both NaCl exposures and water exposures. The samples that absorbed the least amount of moisture under both exposures were the reference samples. This result was somewhat unexpected due to the increase in matrix density due to particle packing. Reference samples had the same amount of PCE as samples containing CNF; however, the addition of CNF reduced the workability of the sample. Reduction in workability could have lead to more void spaces and, therefore, a higher absorption of water.

5.2.2.1 Effects of moisture on conductivity

Samples were exposed to water for 24 hours to determine the effect of water exposure on the conductivity in the samples tested. Exposing the samples to the different moisture conditions increased the conductivity of the samples for all samples tested. Due to water exposure, the conductivity increased by 12.88, 16.62, and 23.55% for reference-PVA-FRC, CNF-PVA-FRC, and CNT-PVA-FRC, respectively. The increased conductivity was more evident in the presence of CNFs/CNTs. Samples containing CNTs increased conductivity of samples showing that these materials have higher electrical conductivity than both CNFs and reference materials.

5.2.2.2 Effects of Na chlorides on conductivity

Samples that were exposed to 2% NaCl solution for 24 hours increased the conductivity for all samples tested. Exposing the samples to chloride conditions increased the conductivity by 19.77, 27.69, and 29.64% for reference-PVA-FRC, CNF-PVA-FRC, and CNT-PVA-FRC, respectively. The increased conductivity was more evident in the presence of CNFs and CNTs. Samples containing CNTs had the largest increase in conductivity which was expected due to the higher electrical properties associated with CNTs compared to CNFs. Increased conductivity of CNTs is due to the production process of the material.

5.3 Crack detection

Samples were loaded until failure using a universal testing machine (Instron 3369). Two loading conditions were used to test the proposed method of NDT testing. Loading conditions considered are flexural and tensile loading. Changes in conductivity were observed during loading to aid in the detection of crack formation.

Crack detection was found to be possible through two methods of data analysis. The two methods used are known as the relative and differential response methods as defined in section 4.1.4. The piezioresistivity and conductivity of PVA-FRC materials change in proportion to strain so the proposed relative conductivity method allowed for crack detection of FRC. When comparing the data for the relative conductivity C/C_0 with the stress-strain curve, the strong correlation between the cracking of the FRC and the relative change in conductivity can be observed.

5.3.1 Tensile loading

Testing samples under tensile loading to determine whether cracks can be observed was a focus in this study. The testing procedure for tensile loading is described in section 3.4.4.

5.3.1.1 External electrodes

In the tensile loading test, external electrodes provided a useful tool for the crack detection through monitoring the changes in conductivity. Samples were first analyzed using the relative method for conductivity analysis. The conductivity response of FRC remains constant until it suffers its initial crack for all sample compositions. Before the samples cracked, the conductivity had a relatively low, but distinctive slope. The slope of conductivity, however, changes drastically at the corresponding strain once the sample suffers its first crack, indicating post-cracking response. The relative and differential conductivities are shown in Figure 44, Figure 45, and Figure 46 for reference FRC, CNF-PVA-FRC, and CNT-PVA-FRC, respectively.

When comparing the data for the fractional change in conductivity with the stress-strain curve, there is match between the matrix cracking and the fractional change in conductivity. When the first major crack appears in the reference FRC at a strain of 0.004 mm/mm, the differential conductivity has a spike at the same strain (Figure 44). Cracks are voids in the concrete matrix and act as electrical insulators decreasing conductivity [15]. The strong spike in the reference sample for the initial crack is more defined than the flowing cracks experienced by the sample at 0.01 mm/mm (Figure 44),

because the fibers holding the PVA-FRC composite over the cracks are effective insulators reducing the ability of the matrix to conduct current.

Figure 45 shows the performance of CNF-PVA-FRC material. The CNFs were used to increase the self-sensing ability of the cement matrix. The conductivity was observed to remain constant with stress until the first crack formed at a strain of 0.0013 mm/mm (Figure 45). After the first crack, there is a significant change in conductivity rate correlated with the response of cracked matrix. The following major cracks at strains of 0.015 and 0.017 mm/mm (Figure 45) are better defined compared with the reference FRC, which is due to the carbon fibers bridging the cracks in the concrete, lowering the defect sizes and increasing the local conductivity of samples.

Figure 46 shows the performance of CNT-PVA-FRC material. The conductivity was observed to increase with stress at a very low rate until the first crack formed at a strain of 0.008 mm/mm (Figure 46). After the first crack, there is a significant change in conductivity rate correlated with the response of cracked matrix. The following major cracks at strains of 0.01 and 0.014 mm/mm (Figure 46) are better defined compared with the reference FRC, which is due to the carbon nanotubes bridging the cracks in the concrete, lowering the defect sizes and increasing the local conductivity of samples.

The change in differential conductivity of FRC due to cracking was more definite in specimens containing CNF or CNT. The smaller changes in conductivity of CNF-PVA-FRC and CNT-PVA-FRC after the main cracking could be attributed to micro-cracking. The smaller cracks led to a smaller change in conductivity and were less defined than the major cracks. These changes are important for detecting micro-cracks and, therefore, nondestructive monitoring of structures.

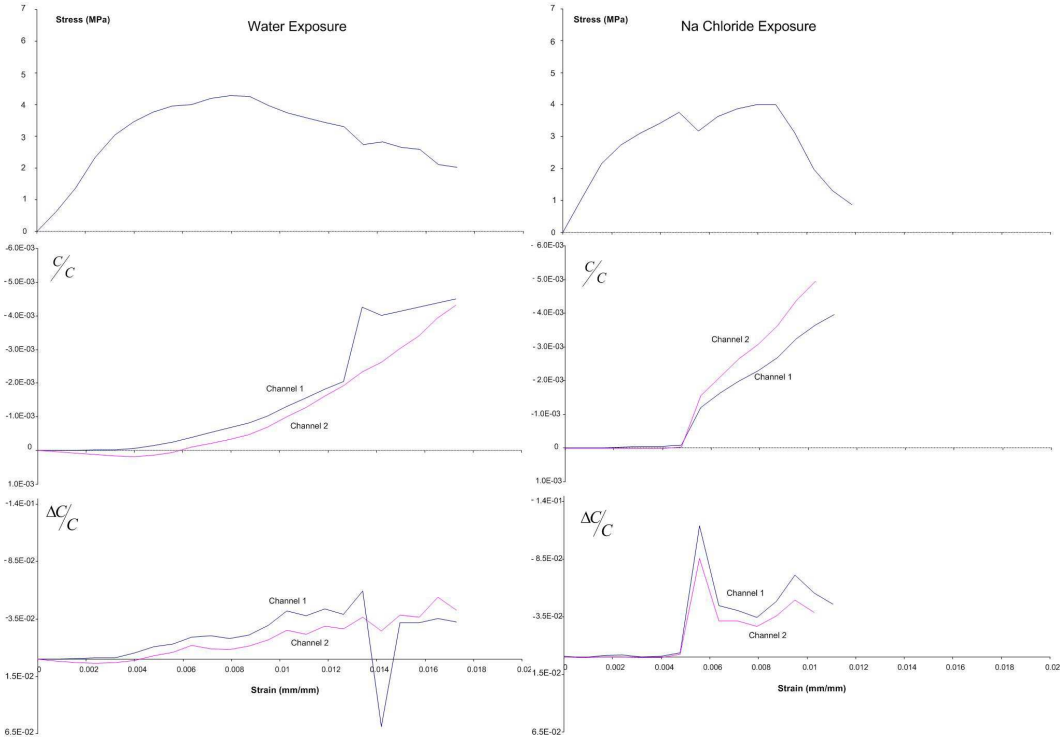

a) b)

Figure 44 The stress-strain performance and relative conductivity (reverse scale) of reference FRC samples after 24h exposure to a) tap water and b) 2% Na chloride solution under tensile loading.

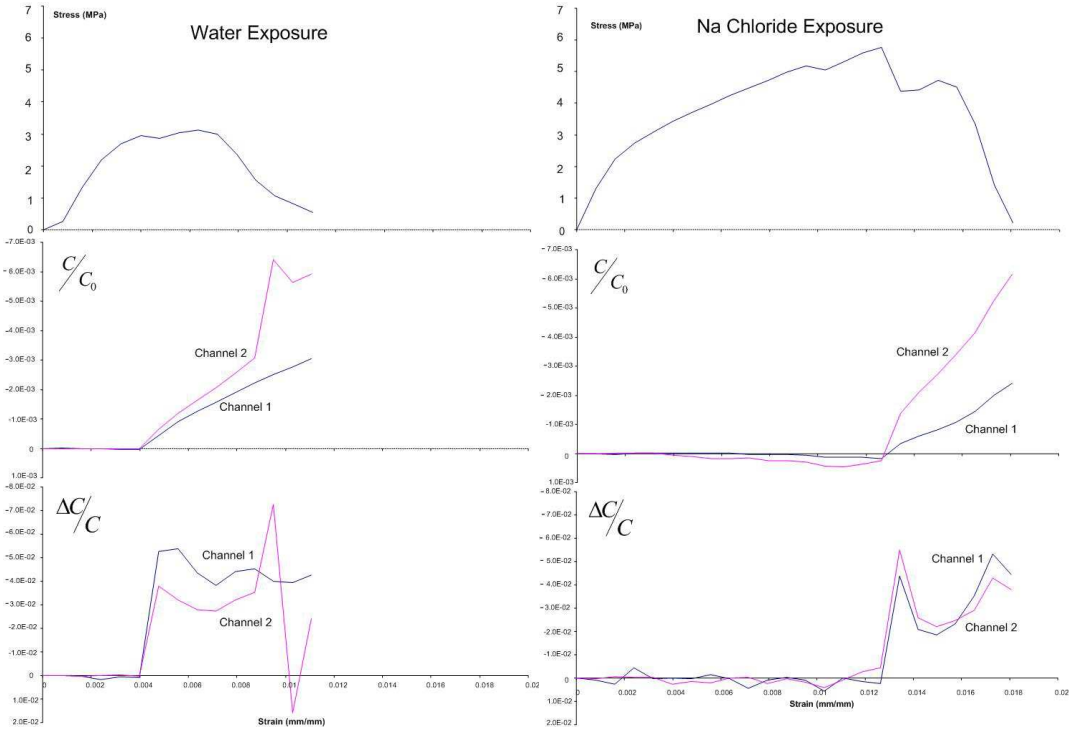

a) b)

Figure 45 The stress-strain performance and relative conductivity (reverse scale) of CNF-PVA-FRC samples after 24h exposure to a) tap water and b) 2% Na chloride solution under tensile loading.

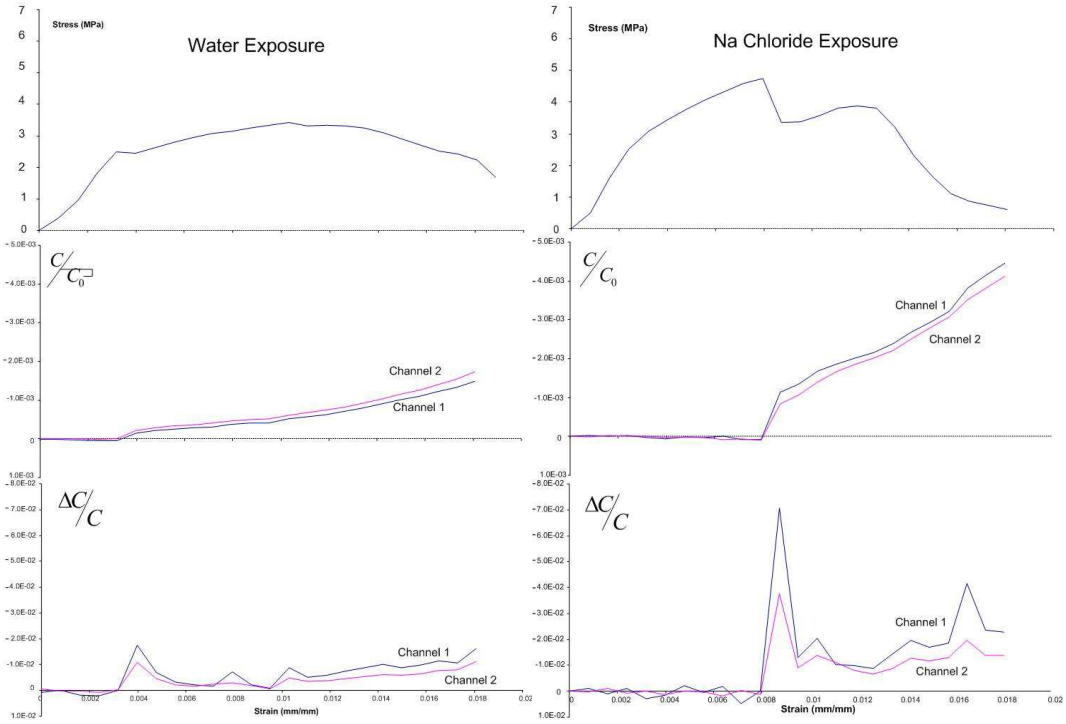

a) b)

Figure 46 The stress-strain performance and relative conductivity (reverse scale) of CNT-PVA-FRC samples after 24h exposure to a) tap water and b) 2% Na chloride solution under tensile loading.

5.3.1.2 Embedded electrodes

Embedded electrodes had much of the same results when compared to the external electrodes. This proves that both methods for electrode placement are viable options for conductivity readings for the use in crack detection. Reference-PVA-FRC, CNF-PVA-FRC, and CNT-PVA-FRC all demonstrated the ability to detect crack formation through the use of embedded electrodes for both relative and differential methods of conductivity analysis. Figure 47, Figure 48, and Figure 49 display the results for relative and differential methods for reference FRC, CNF-PVA-FRC, and CNT-PVA-FRC, respectively.

In general, samples using embedded electrodes had a change in slope when there was a fracture of the concrete matrix when analyzing samples for relative changes in conductivity. Some samples using this method of detection had a harder time making these observations probably due to the fact that the materials were attached to the fiber glass mesh. The mesh may not have had a perfect bond with the surrounding concrete and could have had some slipping action when loaded under tension. However, this behavior was only observed in one sample so it's not expected to be a common occurrence.

The differential method of monitoring changes in conductivity lead to crack detection in all samples monitored. The samples that were the most sensitive were samples containing CNTs. The increased sensitivity is related to the increased conductivity that is observed with samples containing these materials. The conductive CNTs bridge crack that form in the concrete matrix while allowing for less interruption in electrical conduction. For this reason, smaller cracks are more defined in these samples than reference samples. Figure 49 shows the performance of CNT-PVA-FRC material. The conductivity was observed remain constant with stress until the first crack formed at a strain of 0.01 mm/mm (Figure 49). After the first crack, there is a significant change in conductivity rate correlated with the response of cracked matrix. The following major cracks at strains of 0.02 and 0.018 mm/mm (Figure 49) are also represented in the differential measurements.

When comparing the data for the fractional change in conductivity with the stress-strain curve, there is match between concrete cracking and the fractional change in conductivity. When the first major crack appears in the reference FRC at a strain of 0.01

mm/mm, the differential conductivity has a spike at the same strain (Figure 47). The strong spike in the reference sample for the initial crack is more defined than the flowing cracks experienced by the sample at 0.025 mm/mm (Figure 47), because the fibers holding the PVA-FRC composite over the cracks are effective insulators reducing the ability of the matrix to conduct current.

The change in differential conductivity of FRC due to cracking was more definite in specimens containing CNF or CNT. The smaller changes in conductivity of CNF-PVA-FRC and CNT-PVA-FRC after the main cracking could be attributed to micro-cracking or slipping of the fiberglass mesh. The carbon fiber mesh used in this work was included to keep the steel fibers in place during the placement of the concrete. The mesh provided additional strength to the sample of the purpose of monitoring samples loaded in tension; however, it also may have lead to additional readings to occur due to the damage done to the mesh or the debonding of the mesh and mortar due to the tensile applied load.

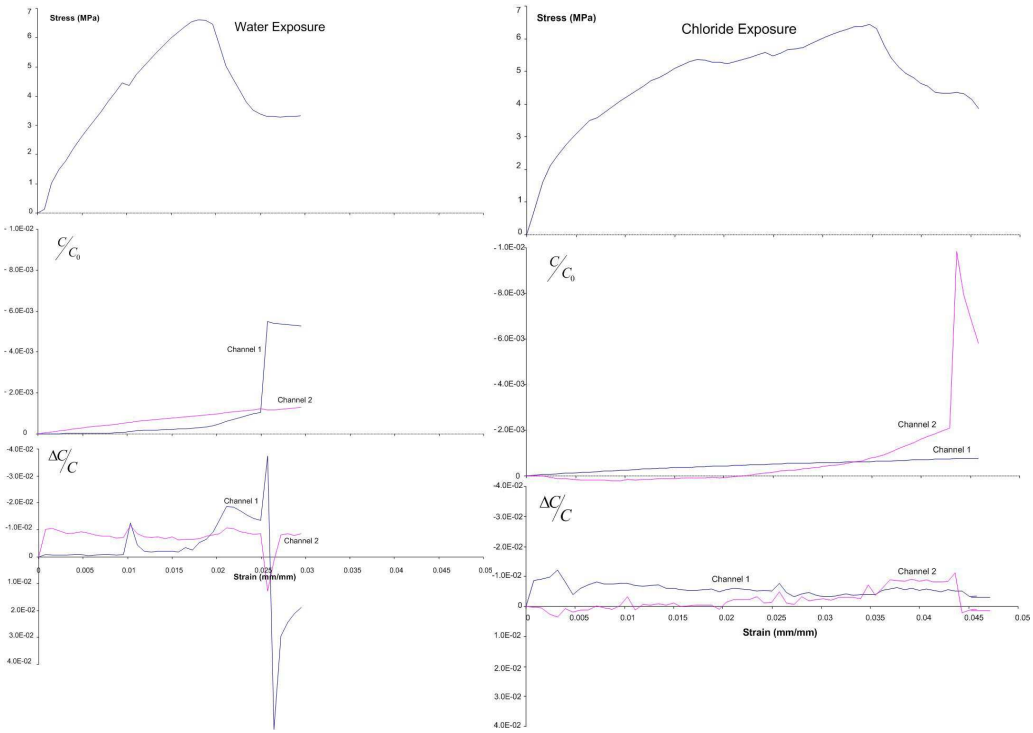

a) b)

Figure 47 The stress-strain performance and relative conductivity (reverse scale) of reference FRC samples after 24h exposure to a) tap water and b) 2% Na chloride solution under tensile loading.

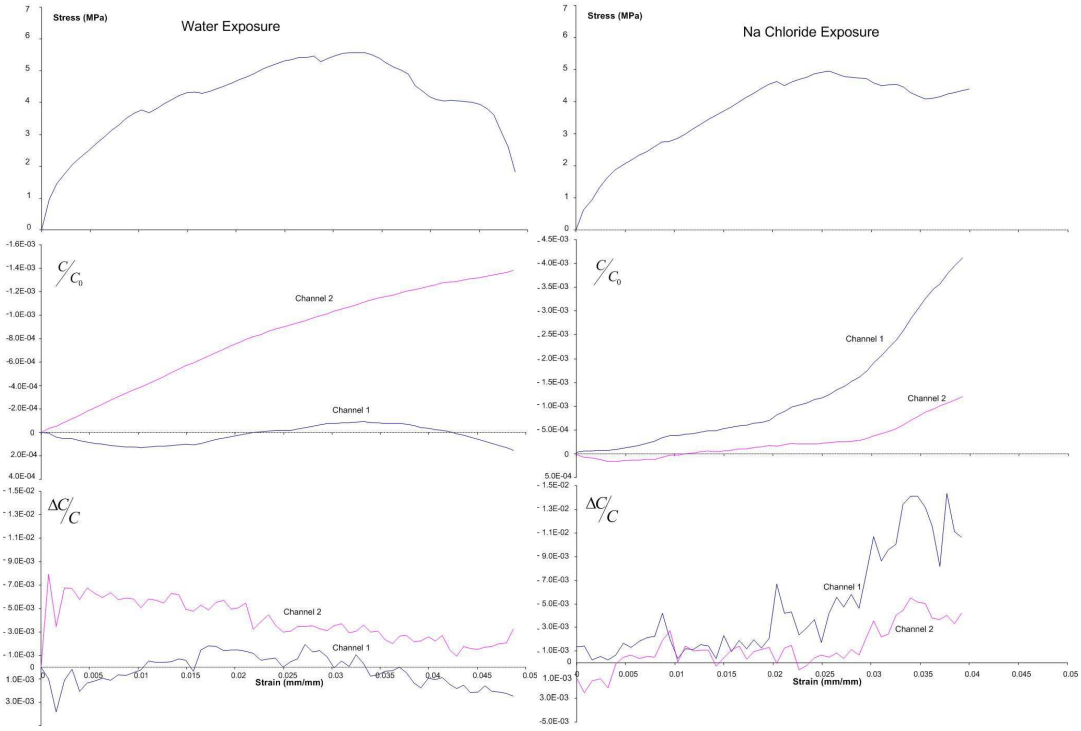

a) b)

Figure 48 The stress-strain performance and relative conductivity (reverse scale) of CNF-PVA-FRC samples after 24h exposure to a) tap water and b) 2% Na chloride solution under tensile loading.

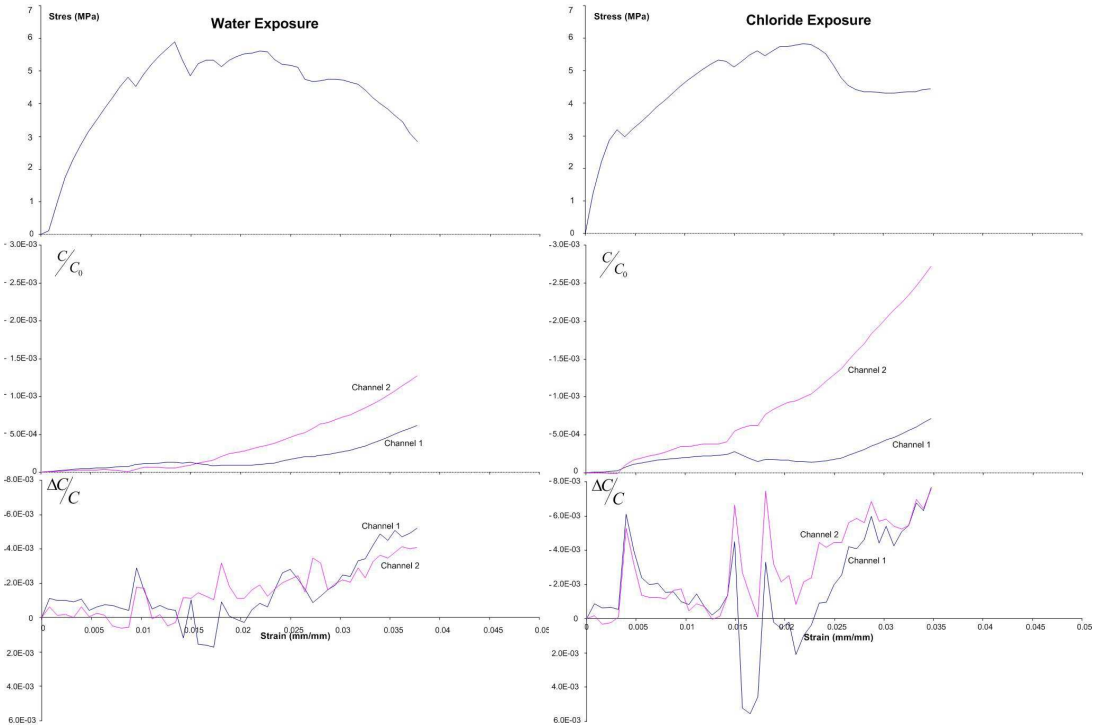

a) b)

Figure 49 The stress-strain performance and relative conductivity (reverse scale) of CNT-PVA-FRC samples after 24h exposure to a) tap water and b) 2% Na chloride solution under tensile loading.

5.3.2 Flexural loading

Through the testing of the samples under flexural loading (loading rate of 1.2 mm/minute) it was observed that the loading style and electrode type did not affect the materials ability to detect cracks. The two methods described for monitoring crack formation through measuring the changes in conductivity through the mortar matrix yielded results that strongly correlate with formation

5.3.2.1 External electrodes

Section 4.4 describes how the process was conducted to analyze the materials under flexural loading using external electrodes. Figure 50, Figure 51, and Figure 52 represent the measurements made for crack formation under flexural loading for reference, CNF, and CNT samples, respectively for external electrodes. In the main study, it was confirmed that the changes in conductivity correlated with crack formation under flexural loading as concluded in the preliminary study.

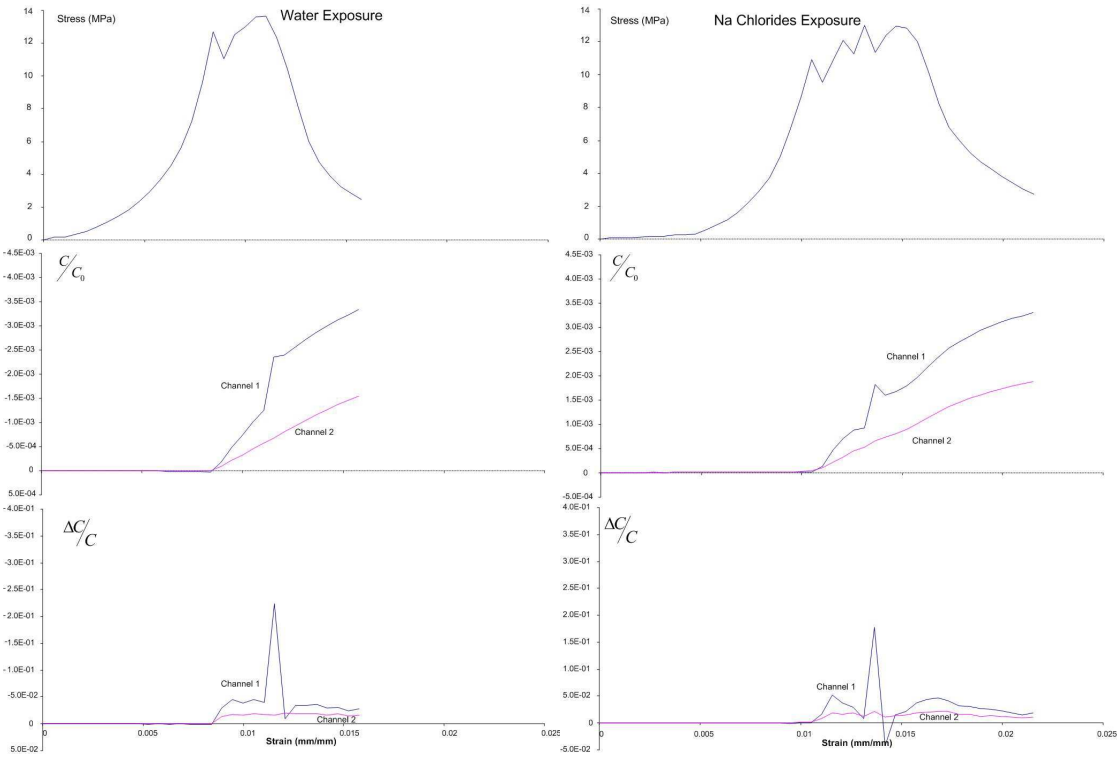

a) b)

Figure 50 The stress-strain performance and relative conductivity (reverse scale) of reference FRC samples after 24h exposure to a) tap water and b) 2% Na chloride solution under flexural loading.

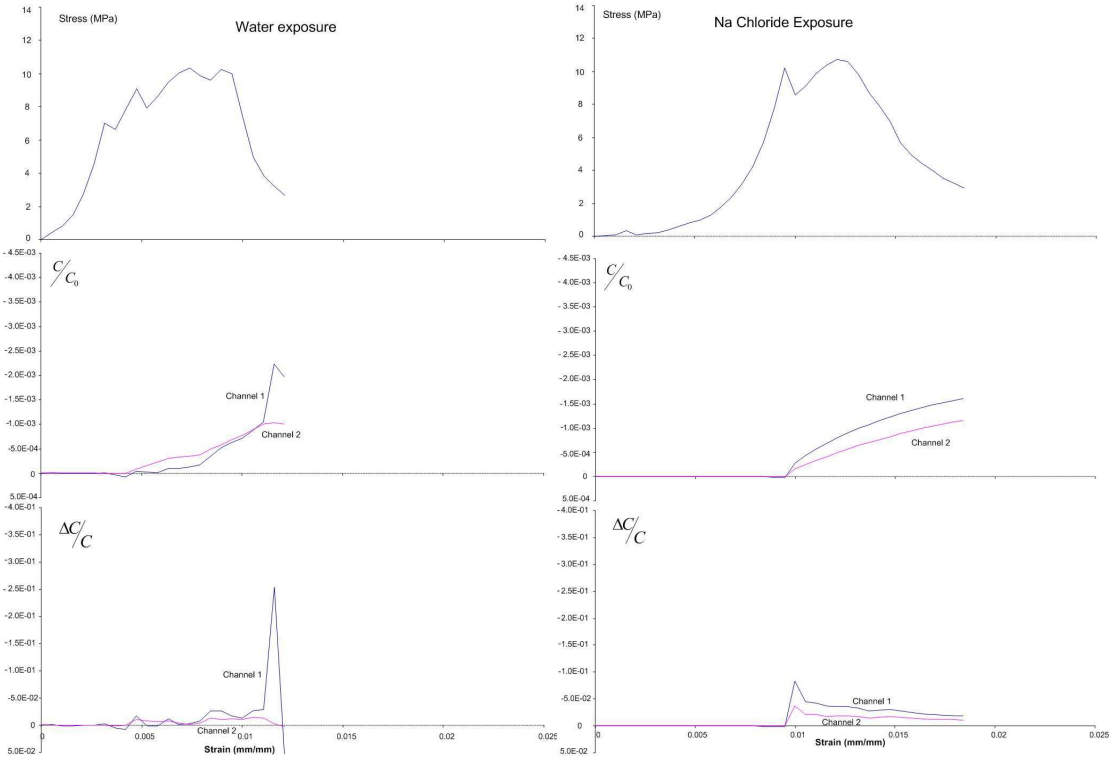

a) b)

Figure 51 The stress-strain performance and relative conductivity (reverse scale) of CNF-PVA-FRC samples after 24h exposure to a) tap water and b) 2% Na chloride solution under flexural loading.

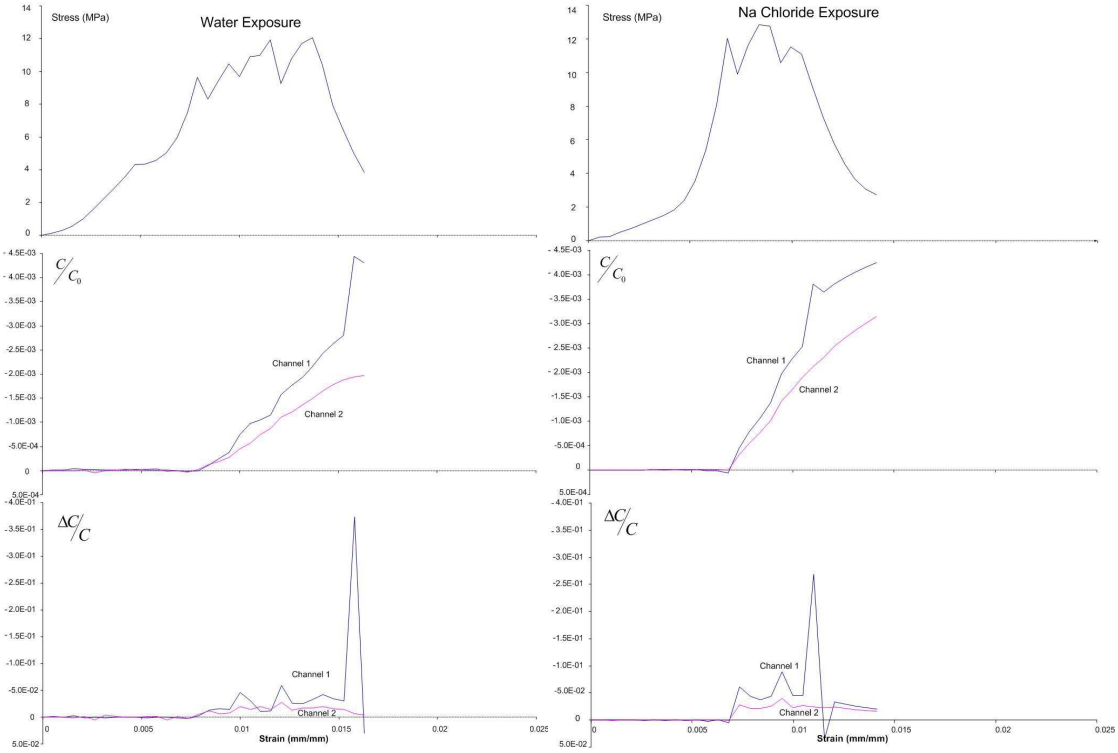

a) b)

Figure 52 The stress-strain performance and relative conductivity (reverse scale) of CNT-PVA-FRC samples after 24h exposure to a) tap water and b) 2% Na chloride solution under flexural loading.

5.3.2.2 Embedded electrodes

Embedded electrodes loaded under flexural loading demonstrated the same abilities to detect crack formation. Under flexural loading, the samples experienced changes in conductivity that correlated crack formations. The changes in conductivity are due to the void spaces formed due to cracking. Figure 53, Figure 54, and Figure 55 represent samples with embedded electrodes. A large change in conductivity in the final cracking event for CNF-PVA-FRC exposed to tap water created issues in comparing conductivity changes in samples exposed to NaCl on the same scale. Figure 54 includes

an additional graph for with an adjusted scale to view crack formations under flexural loading for CNF-PVA-FRC exposed to NaCl.

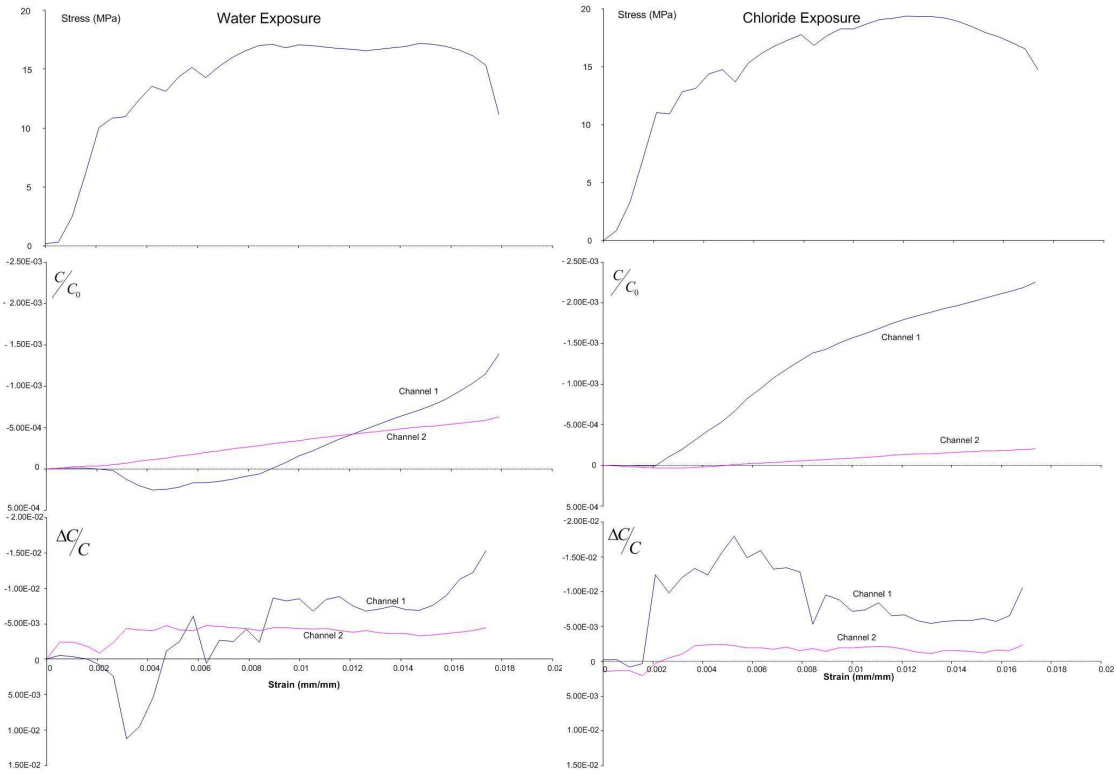

a) b)

Figure 53 The stress-strain performance and relative conductivity (reverse scale) of reference FRC samples after 24h exposure to a) tap water and b) 2% Na chloride solution under flexural loading.

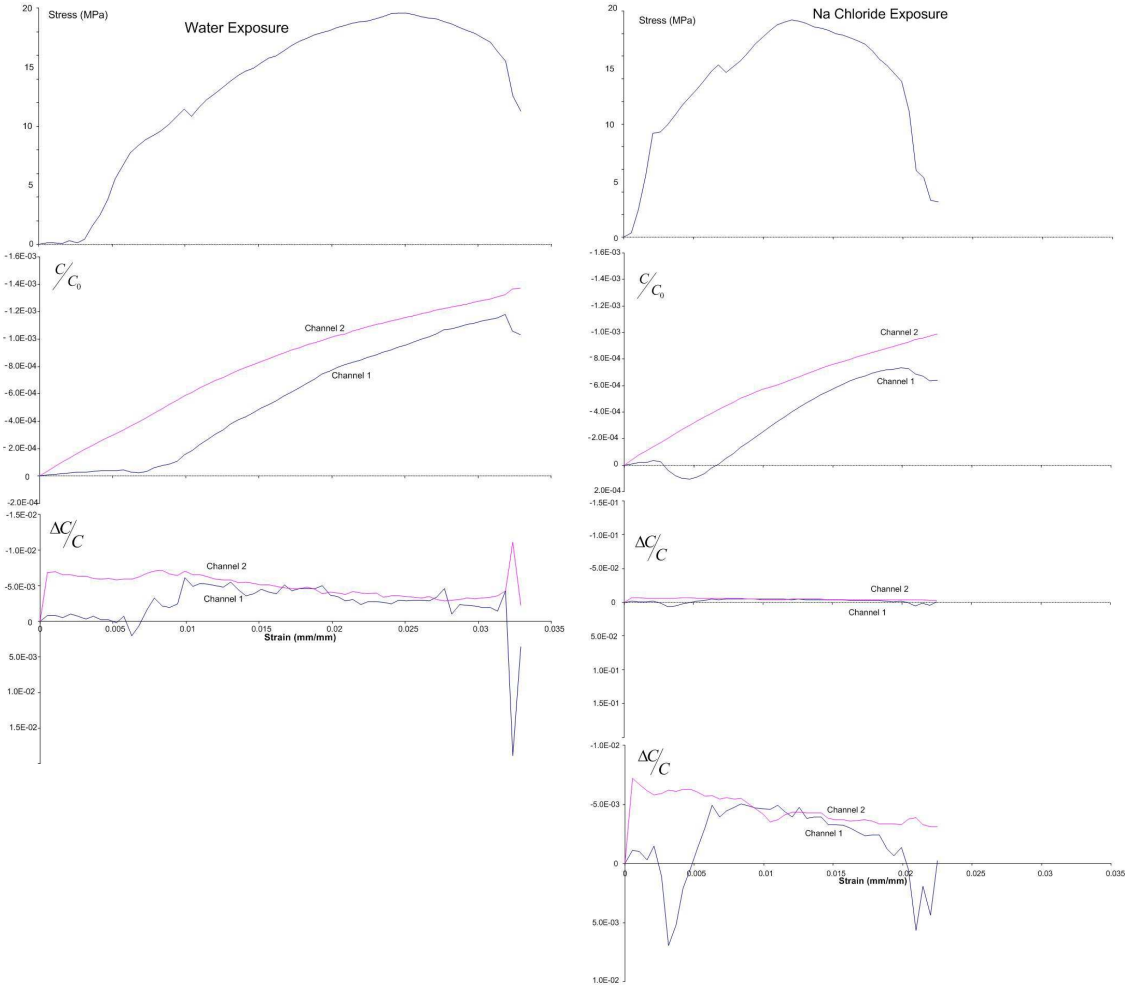

a) b)

Figure 54 The stress-strain performance and relative conductivity (reverse scale) of CNF-PVA-FRC samples after 24h exposure to a) tap water and b) 2% Na chloride solution under flexural loading.

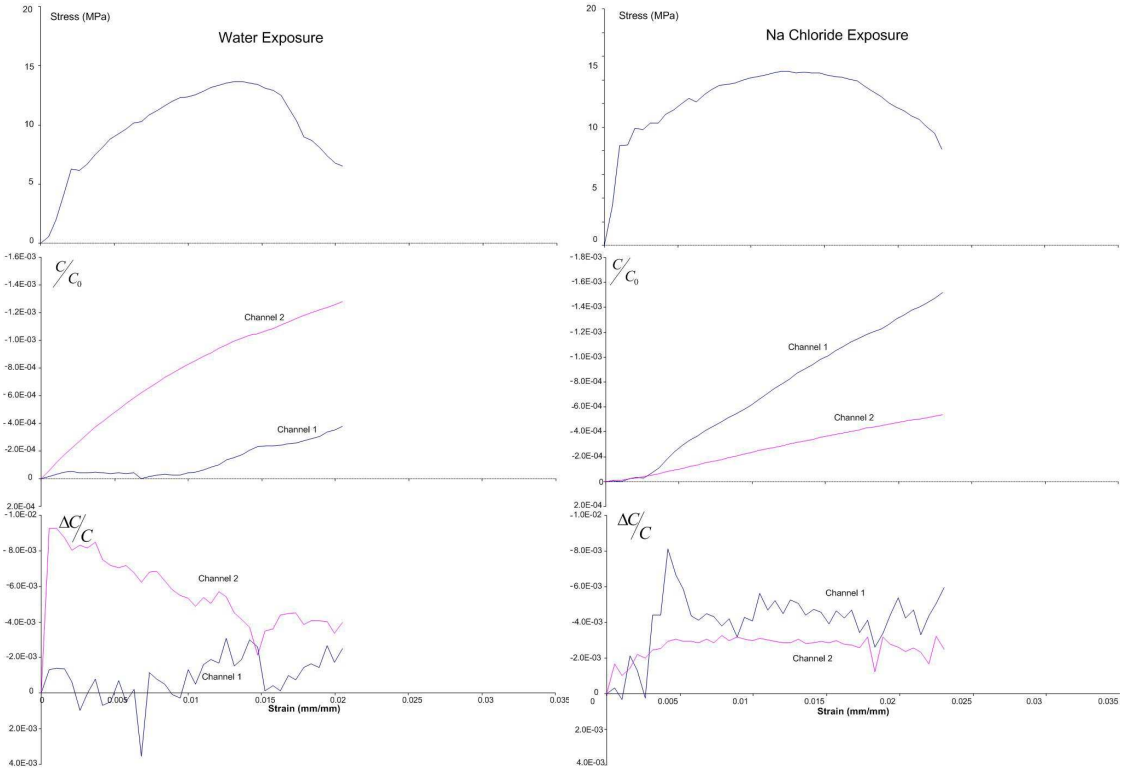

a) b)

Figure 55 The stress-strain performance and relative conductivity (reverse scale) of CNT-PVA-FRC samples 24h exposure to a) tap water and b) 2% Na chloride solution under flexural loading.

5.4 Effects of exposure type on conductivity

Exposing samples to moisture affected the materials ability to conduct electricity. Tap water has the ability to conduct electricity due to the impurities in the water's composition. The 2% NaCl by weight of tap water has the ability to conduct electricity due to the presence of chloride ions. This ability was demonstrated in the charts for both the external and embedded sensors shown in sections 5.3.1 and 5.3.2. The differential conductivity was observed to have higher differential changes in conductivity for all samples observed except the reference material for embedded sensors.

The samples exposed to chlorides and water is compared to determine how the exposure type affects the conductivity. Reference, CNF, and CNT samples were compared to determine differences in conductivity when comparing chlorides to water exposure are 1.12, 1.00, and 0.16% for external electrodes. For the embedded electrodes the difference in conductivity for reference, CNF, and CNT were 0.50, 0.76, and 0.60% respectively. The increase in conductivity was able to show that this method is effective for chloride detection in mortar.

6 Conclusions

The idea to have safe and constant monitoring of concrete structures is not a new concept. Past research has yielded nondestructive techniques for monitoring crack formation in concrete structures that are expensive and limited in their use. The developed concept allows for the constant NDT monitoring of concrete structures in a cost-effective manner.

Cost reduction for the proposed NDT system was achieved in multiple ways. The largest cost savings achieved by allowing this system to be included in a structure without the need to change the construction process that the industry has become accustomed to. This includes using standard formwork for concrete structures as well as standard rebar layouts and other standard construction techniques. This applies for both embedded and external electrodes used for conductivity measurements. Embedded electrodes can be simple strips of stainless steel, as used in this experiment, limiting the inclusion of additional materials in a formwork that may already be crowded. The external electrodes do not require a change in construction philosophy since the electrodes would be included after the construction of the structural element was finished or added to an existing structure. Furthermore, the developed FRC material can be used in a form of stress sensing skin with thickness of 2 – 15 mm incorporated into existing concrete.

The proposed technique saves in cost when compared to other techniques while in service in addition to the savings during construction. This technique does not require the use of expensive equipment for the monitoring of structural elements. Conductivity readings are conducted through the use of a simple data acquisition system connected to

simple electrodes. The proposed concept has cost savings in that it does not require a trained professional to make the observations en situ.

Through the experimental work, it was determined that crack detection through the monitoring of conductivity is a viable NDT technique. Concrete, especially PVA-FRC, has the ability to make the required observations without the inclusion of CNTs or CNFs. For this reason, the inclusion of this NDT technique can be done years after the initial construction of the structure through the use of external electrodes. Embedding the sensors in concrete can help to protect the samples from environmental damage when included in the design of a concrete structure.

Increasing the sensitivity of measurements was a priority in this work. To increase the sensitivity of the material to detect crack formation and propagation, the addition of electrically conductive fibers such as carbon nanotubes and carbon nanofibers to the concrete matrix was used. The CNFs/CNTs are used to bridge cracks that form in the mortar matrix to allow for the formation of smaller cracks through the concrete structure increasing the strength of a sample through strain hardening. The multi-crack forming will increase the ductility of the material and decrease the possibility of a brittle failure in the structural element.

In addition to the PVA fibers, the electrically conductive CNFs and CNTs were used to improve the response of the material. Crack bridging by electrically conductive fibers improved the detection of the change in conductivity vs. PVA fibers.

Polarization in electrical readings is a limiting factor in most techniques for conductivity monitoring. This work allowed for the exclusion of effects of polarization effects by analyzing the change in conductivity instead of monitoring the conductivity.

Direct measurements of conductivity would include polarization and would make the detection of cracks much challenging. Comparing readings to previous readings allowed for polarization effects to be neglected and cracks are directly measured through the differential and relative techniques proposed in this work.

The fibers used in this work are often hard to disperse within the mix. Dispersion of CNFs and CNTs was greatly improved through the use of ultrasonic mixing combined with the use of superplasticizer. To break up the additional Van der Waals forces holding CNTs, the inclusion of a small portion of the sand increased the ability of the material to be dispersed in a given medium.

The monitoring of NaCl penetration to a mortar element through conductivity measurements was shown to be feasible through this work. The electromechanical response of reference FRC subjected to water and Na chlorides was similar to CNF-PVA and CNT-PVA based FRC. PVA based FRC exposed to the 2% NaCl solution demonstrated higher changes in differential conductivity than those exposed only to water. This change in relative conductivity can be observed most definitively at the first crack in the concrete matrix and can be used for chloride detection. Generally, samples exposed to Na chlorides had a steeper slope of relative conductivity than the sample exposed only to water. The results of this study demonstrated the ability of self-sensing CNF/CNT-PVA based FRC to provide safe, systematic, and nonbiased monitoring of concrete structures.

Future work

The reported project has demonstrated the feasibility of monitoring structures for the formation of cracks and chloride penetration through the use of conductivity measurements. It would be beneficial to this project would be to prove the penetration of chloride ions to the concrete matrix through Scanning Electron Microscope (SEM) and Energy Diffraction Scattering (EDS). Future work would also include using SEM to prove the equal dispersion of CNT and CNF to the concrete matrix. The work done with this technique has been included in small samples exposed only to loads subjected to failure. Including this technique in a future structure or attaching electrodes to monitor existing structural elements would prove the practical applicability to improve structural integrity and reduce the inspection costs.

References

1. Banthia, N. (2009). “Fiber Rienforced Concrete for Sustainable and Intelligent Infrastructure.” SBEIDCO – 1st International Conference on Sustainable Built Enviornment Infrastructures in Develping Contries ENSET Oran (Algeria): 14
2. Boyd, A. “Nondestructive Testing for Advanced Monitoring and Evaluation of Damage in Concrete Materials Florida DOT”.
3. Cao, J. Y. and D. D. L. Chung (2004). "Electric polarization and depolarization in cement-based materials, studied by apparent electrical resistance measurement." Cement and Concrete Research **34**(3): 481-485.
4. Chacko, Rose Mary, Nemkumar Banthia, and Aftab A. Mufti. "Carbon-fiber-reinforced Cement-based Sensors." *Canadian Journal of Civil Engineering* 34.3 (2007): 284-90.
5. Chen, B. and J. Y. Liu (2008). "Damage in carbon fiber-reinforced concrete, monitored by both electrical resistance measurement and acoustic emission analysis." Construction and Building Materials **22**(11): 2196-2201.
6. Chiarello, M. and R. Zinno (2005). "Electrical conductivity of self-monitoring CFRC." Cement & Concrete Composites **27**(4): 463-469.
7. Chung, D. D. L. (2002). "Piezoresistive cement-based materials for strain sensing." Journal of Intelligent Material Systems and Structures **13**(9): 599-609.
8. Chung, X. F. a. D. D. L. (1995). "Contact electrical resistivity between cement and carbon fiber: its decrease with increasing bond strength and its increase during fiber pull-out" Cement and Concrete Research **25**(7): 1391-1396.
9. Chung, D. D. L. (2002). "Piezoresistive cement-based materials for strain sensing." Journal of Intelligent Material Systems and Structures **13**(9): 599-609.
10. Chung, D. D. L. (2005). "Dispersion of short fibers in cement." Journal of Materials in Civil Engineering **17**(4): 379-383.
11. Chung, X. F. a. D. D. L. (1995). "Contact electrical resistivity between cement and carbon fiber: its decrease with increasing bond strength and its increase during fiber pull-out" Cement and Concrete Research **25**(7): 1391-1396.
12. Collins, Frank, John Lambert, and Wen Hui Duan. "5. The Influences of Admixtures on the Dispersion, Workability, and Strength of Carbon Nanotube–OPC Paste Mixtures." *Cement & Concrete Composites* (2011): 201-07.
13. Deng, Z. C. (2005). "The fracture and fatigue performance in flexure of carbon fiber reinforced concrete." Cement & Concrete Composites **27**(1): 131-140.
14. Hilding, Jenny, Eric A. Grulke, Z. George Zhang, and Fran Lockwood. "Dispersion of Carbon Nanotubes in Liquids." *Journal of Dispersion Science and Technology* 24.1 (2003): 1-41.
15. Hou, T. C. and J. P. Lynch (2005). "Conductivity-based strain monitoring and damage characterization of fiber reinforced cementitious structural components"

Proceedings of SPIE 12th Annual International Symposium on Smart Structures and Materials

16. Hou, T. C. and J. P. Lynch (2009). "Electrical Impedance Tomographic Methods for Sensing Strain Fields and Crack Damage in Cementitious Structures." Journal of Intelligent Material Systems and Structures **20**(11): 1363-1379.
17. Juan, Li, Jinping Suo, and Runzhi Deng. "Structure, Mechanical, and Swelling Behaviors of Poly(vinyl Alcohol)/SiO2 Hybrid Membranes." *Journal of Reinforced Plastics and Composites* (2009)
18. Karhunen, K., A. Seppanen, A. Lehikoinen, P. J.M. Monteiro, J. P. Kaipio (2010). "Electrical Resistance Tomography imaging of concrete." Cement and Concrete Research **40**(1): 137-145.
19. K. Sakata, M. A. El-Wafa and T. Ayano, "Mixing Effects of Different Sizes of Synthetic Fibers on Concrete," *ACI International Conference on Durability of Concrete*, Vols. SP-212-36, pp. 571-578, 2003
20. Khanna, Vikas, Bhavik R. Bakshi, and L. James Lee. "Carbon Nanofiber Production." *Journal of Industrial Ecology* 12.3 (2008): 394-410.
21. Konsta-Gdoutos, Maria S., Zoi S. Metaxa, and Surendra P. Shah. "Highly Dispersed Carbon Nanotube Reinforced Cement Based Materials." *Cement and Concrete Research* 40.7 (2010): 1052-059.
22. Li, J., J. P. Suo, R. Deng (2010). "Structure, Mechanical, and Swelling Behaviors of Poly(vinyl alcohol)/SiO(2) Hybrid Membranes." Journal of Reinforced Plastics and Composites **29**(4): 618-629.
23. Metaxa, Z.S., M.S. Konsta-Gdoutos, S.P. Shah. "Mechanical Properties and Nanostructure of Cement-Based Materials Reinforced with Carbon Nanofibers and Polyvinyl Alcohol (PVA) Microfibers." Infrastructure Technology Institute
24. Nili, Mahmoud, and V. Afroughsabet. "Combined Effect of Silica Fume and Steel Fibers on the Impact Resistance and Mechanical Properties of Concrete." *International Journal of Impact Engineering* 37.8 (2010): 879-86.
25. Nevers, D., J. Zhao, K. Sobolev, G. Hanson (2011). "Investigation of strain-sensing materials based on EM surface wave propagation for steel bridge health monitoring." Construction and Building Materials **25**(7): 3024-3029.
26. Olivito, R.S., and F.A. Zuccarello. "An Experimental Study on the Tensile Strength of Steel Fiber Reinforced Concrete." *Composites Part B: Engineering* 41.3 (2010): 246-55.
27. Ozyurt, N., L. Y. Woo, T. Mason, and S. P. Shahet (2006). "Monitoring fiber dispersion in fiber-reinforced cementitious materials: Comparison of AC-impedance spectroscopy and image analysis." Aci Materials Journal **103**(5): 340-347.
28. Pyrograf-III carbon nanofiber: http://pyrografproducts.com/Merchant5/merchant.mvc?Screen=cp_nanofiber

29. Rastogi, Richa, Rahul Kaushal, S.K. Tripathi, Amit L. Sharma, Inderpreet Kaur, and Lalit M. Bharadwaj. "Comparative Study of Carbon Nanotube Dispersion Using Surfactants." *Journal of Colloid and Interface Science* 328.2 (2008): 421-28.

30. Sanchez, Florence, and Chantal Ince. "Microstructure and Macroscopic Properties of Hybrid Carbon Nanofiber/silica Fume Cement Composites." *Composites Science and Technology* 69.7-8 (2009): 1310-318.

31. Sung-Ho, Tae, and Rak-Hyun Kim. "A Study on Improvement of Durability of Reinforced Concrete Structures Mixed with Natural Inorganic Minerals." *Construction and Building Materials* (2011): 4263-270.

32. Vaisman, L., H. Wagner, and G. Marom. "The Role of Surfactants in Dispersion of Carbon Nanotubes." *Advances in Colloid and Interface Science* 128-130 (2006): 37-46.

33. V. C. Li, "Engineered Cementitious Composites (ECC)- Tailored Composites through Micromechanical Modeling".

34. The influence of steel slag on the hydration of cement during the hydration process of complex binder Wang Qiang

35. Wang, Calvin S., Fan Wu, and Fu-Kuo Chang. "Structural Health Monitoring from Fiber-reinforced Composites to Steel-reinforced Concrete." *Smart Materials and Structures* (2001): 548-52.

36. Wang, S., D.D.L. Chung (2000). "Electrical behavior of carbon fiber polymer matrix composites in the through-thickness direction" Journal of Materials Science **35**: 91-100.

37. Wang, W., S. Wu, and H. Dai. "Fatigue Behavior and Life Prediction of Carbon Fiber Reinforced Concrete under Cyclic Flexural Loading." *Materials Science and Engineering: A* 434.1-2 (2006): 347-51.

38. Wang, Dan, Wen-Xi Ji, Zi-Chen Li, and Liwei Chen. "A Biomimetic “Polysoap” for Single-Walled Carbon Nanotube Dispersion." *Journal of the American Chemical Society* 128.20 (2006): 6556-557.

39. Wen, S. H. and D. D. L. Chung (2000). "Damage monitoring of cement paste by electrical resistance measurement." Cement and Concrete Research **30**(12): 1979-1982.

40. Wen, S. H. and D. D. L. Chung (2001). "Effect of stress on the electric polarization in cement." Cement and Concrete Research **31**(2): 291-295.

41. Wen, S. H. and D. D. L. Chung (2001). "Electric polarization in carbon fiber-reinforced cement." Cement and Concrete Research **31**(1): 141-147.

42. Wen, S. H. and D. D. L. Chung (2006). "Effects of strain and damage on strain-sensing ability of carbon fiber cement." Journal of Materials in Civil Engineering **18**(3): 355-360.

43. Wisconsin Department of Transportation, "Transportation Finance Issues; How is transportation money spent?," 2011

44. http://www.buildinggreen.com/features /flyash/appendixa.cfm

45. Titi, Hani, Habib Tabatabai, and Konstantin Sobolev. "FEASIBILITY STUDY FOR A FREEWAY CORRIDOR INFRASTRUCTURE HEALTH MONITORING (IHM) INSTRUMENTATION TESTBED." *National Center for Freight and Infrastructure Research and Education*

46. Wen, S. H. and D. D. L. Chung (2007). "Electrical-resistance-based damage self-sensing in carbon fiber reinforced cement." Carbon **45**(4): 710-716.

47. Yan, Y., A. Neville, and D. Dowson. "Understanding the Role of Corrosion in the Degradation of Metal-on-metal Implants." *Proceedings of the Institution of Mechanical Engineers, Part H: Journal of Engineering in Medicine* 220.2 (2006): 173-80.

48. Yu, Xun, and Eil Kwon. "A Carbon Nanotube/cement Composite with Piezoresistive Properties." *Smart Materials and Structures* 18.5 (2009): 055010.

49. http://www.germann.org

Appendix: Sample polarization

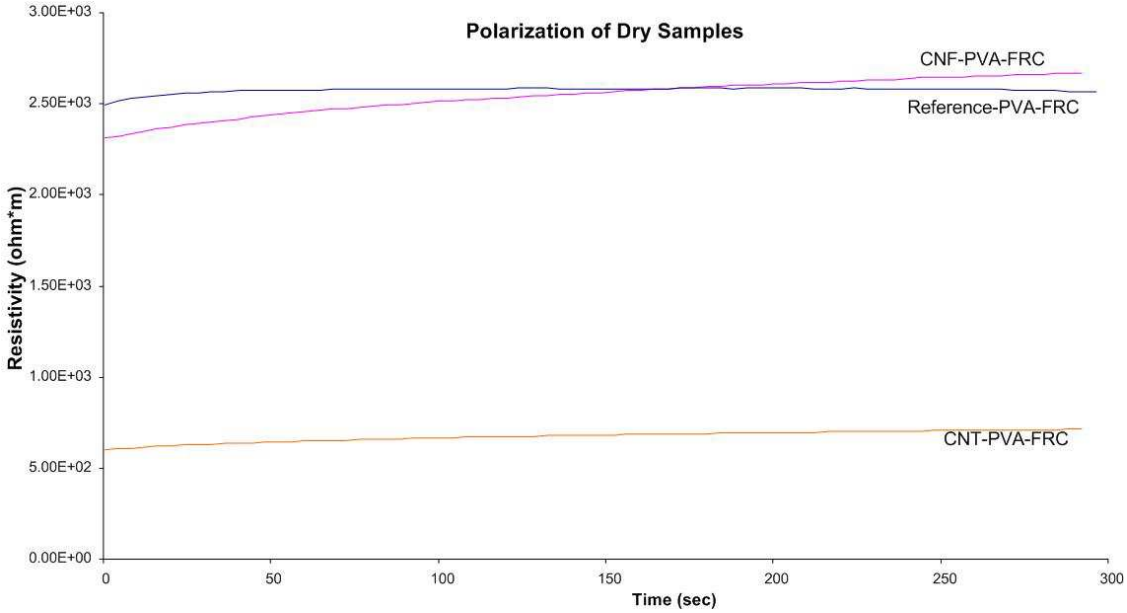

Figure 56 Polarization in dry samples (external electrodes)

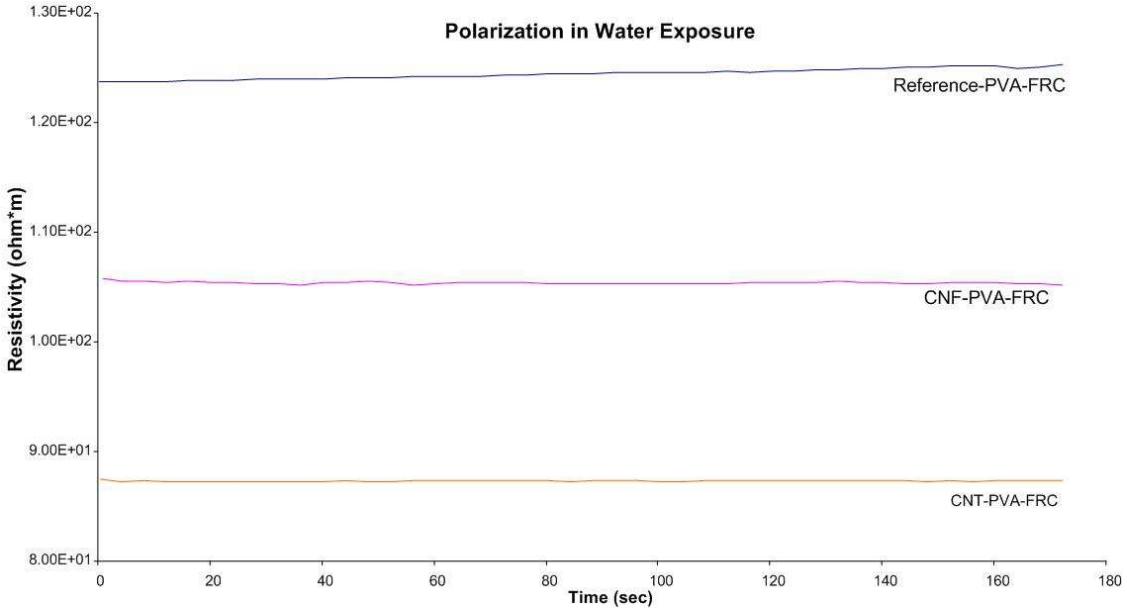

Figure 57 Polarization in samples exposed to tap water (external electrodes)

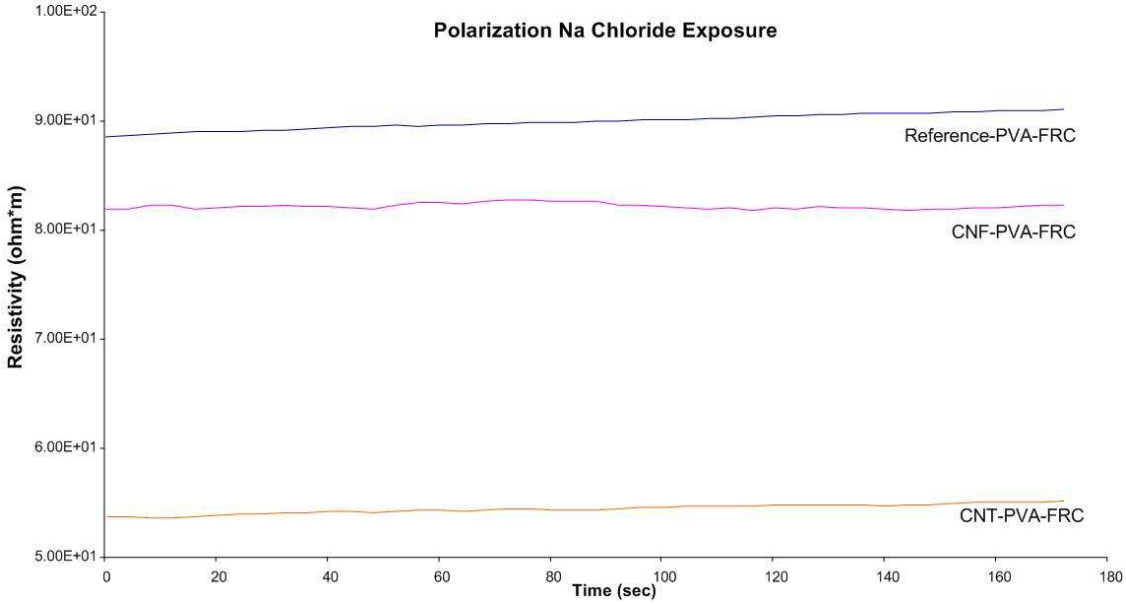

Figure 58 Polarization in samples exposed to NaCl (external electrodes)

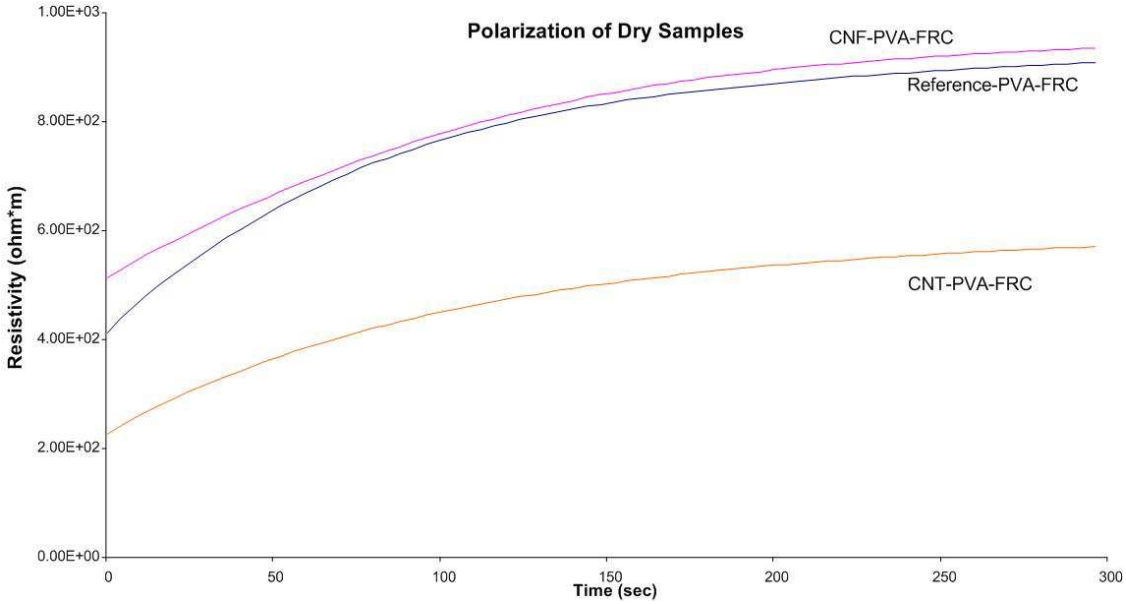

Figure 59 Polarization in dry samples (embedded electrodes)

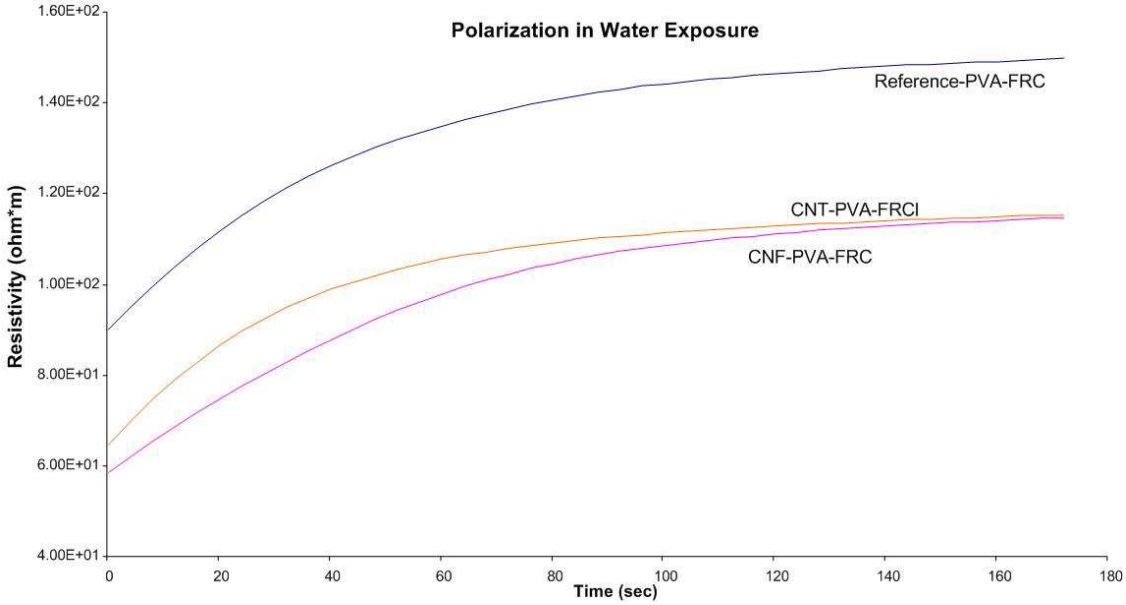

Figure 60 Polarization in samples exposed to tap water (embedded electrodes)

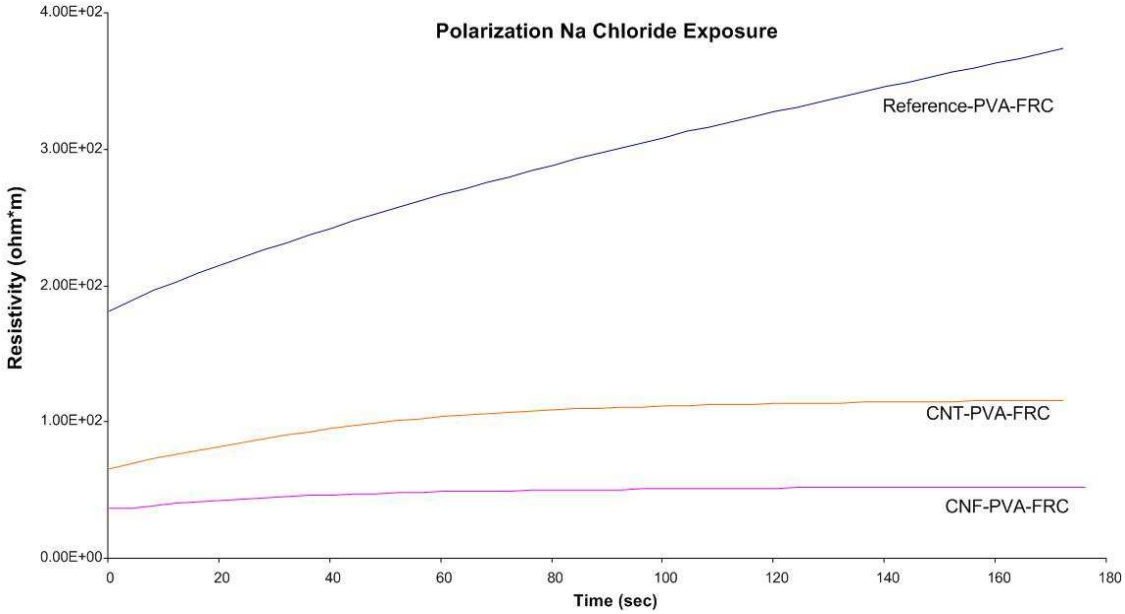

Figure 61 Polarization in samples exposed to NaCl (embedded electrodes)